Experimental Study of Wind Effects on Unglazed Transpired Collectors

Neetha Vasan

A Thesis
In
The Department
of
Building, Civil and Environmental Engineering

Presented in Partial Fulfillment of the Requirements
for the Degree of Master of Applied Science (Building Engineering) at
Concordia University
Montreal, Quebec, Canada

December 2012

CONCORDIA UNIVERSITY
School of Graduate Studies

This is to certify that the thesis prepared

By: Neetha Vasan

Entitled: EXPERIMENTAL STUDY OF WIND EFFECTS ON UNGLAZED TRANSPIRED COLLECTORS

and submitted in partial fulfillment of the requirements for the degree of

Master of Applied Science (Building Engineering)

complies with the regulations of the University and meets the accepted standards with respect to originality and quality.

Signed by the final examining committee:

Dr. Radu Zmeureanu Chair

Dr. Luiz Lopes Examiner

Dr. Andreas Athienitis Examiner

Dr. Theodore Stathopoulos Supervisor

Approved by _____
Chair of Department or Graduate Program Director

_____
Dean of Faculty

Date December 20, 2012

ABSTRACT

Experimental Study of Wind Effects on Unglazed Transpired Collectors

Neetha Vasan

Concordia University, 2012

Unglazed transpired collectors (UTC) are one of the most efficient solar heating technologies available today. High wind velocity affects the performance of UTC; indeed, wind flow on the collector's surface reduces useful heat transferred to the collector fluid by effecting convective heat losses and suction in the pores and thereby outflow from the plenum. Wind does not impinge uniformly on all points on a large area; the velocity distribution depends on wind direction and surroundings.

This thesis presents an experimental study in the Building Aerodynamics Laboratory at Concordia University and an analytical parametric study to assess the effect of wind velocity distribution on UTCs under the influence of approach wind direction and surrounding structures. Velocity measurements from wind tunnel experiments were applied to analytical models of UTC performance evaluation. The common assumption, in UTC analysis, that a reference wind velocity acts uniformly over the UTC surface, as opposed to the more realistic non-uniform distribution, has been shown to underestimate the values of convective heat loss coefficients. The study, when applied to the context of the JMSB solar-wall, indicated a reduction of thermal efficiency by 20 percentage points due to wind. Influence of surroundings on wind flow around the JMSB building has been evaluated. The study casts light on the importance of using actual velocity distributions in UTC analysis.

ACKNOWLEDGEMENT

God Almighty has blessed me with good opportunities and the ability to make the best out of them. My family and loved ones have been my backbone and I would not be where I am today without their moral support and prayers.

Sincere thanks to my supervisor Dr. Theodore Stathopoulos for all my achievements at Concordia University, which would not have been possible without his patience and constant motivation. I am grateful for the encouragement given by Dr. Suresh Kumar who led me to take this route in my academics. Special thanks to Sudeesh Kala for his help and words of advice whenever I was in need of them.

I would like to acknowledge the Center for Zero Energy Buildings (CZEB) that this project is a part of and the awards from Concordia Univeristy and IBPSA, which have been a great motivation. Research input from Dr. Athienitis and James Bambara are much appreciated. Sincere thanks to Tiberiu Aldea, Luc Demers and Joseph Hrib and Tiberiu Aldea for their help at different stages of my work.

Thanks to colleagues turned friends Ting Ting Yang, Costa Kapsis and Diane Bastien and utmost gratitude to Yuxiang Chen, Jose Daniel and Dimitris Ladas, for their valuable inputs that guided me in this research.

TABLE OF CONTENTS

LIST OF FIGURES

LIST OF TABLES

NOMENCLATURE

a,c,e,f	constants in equations (3-5) through (3-7)
c_p	specific heat of air at constant pressure (J/kgK)
D	UTC hole diameter (m)
h_c	convective heat transfer coefficient (W/m^{2}K)
h_r	radiative heat transfer coefficient (W/m^{2}K)
P	UTC hole pitch (m)
Pr	Prandtl number
Q_{conv}	convective heat loss (W/m^2)
Q_{30}, Q_{50}	Convective heat loss at 30% and 50% UTC thermal efficiency (W/m^2)
Re	Reynolds number; $Re_w = \frac{V_{wind}P}{\nu}$ $Re_s = \frac{V_s P}{\nu}$ $Re_b = \frac{V_s P}{\nu\sigma}$ $Re_h = \frac{V_s D}{\nu\sigma}$
t	UTC plate thickness (m)
T_{amb}	temperature of ambient air (^{0}C)
T_{back}	temperature of the air coming out at the back of the collector (^{0}C)
T_{coll}	temperature at the collector surface (^{0}C)
V_{10}	reference wind velocity at 10 m height in the upstream undisturbed flow (m/s), usually measured at a weather station

V_∞	free stream velocity parallel to the UTC (m/s)
V_G	mean wind velocity at gradient height in the ABL (m/s)
V_{loc}	magnitude of local wind velocity vector (m/s)
V_{normal}	component of V_{loc} normal to the building or UTC surface (m/s)
V_{ref}	reference wind velocity measured above the roof (m/s)
V_s	suction velocity in the UTC pores (m/s)
V_{wind}	approach wind velocity (m/s)
V_Z	mean wind velocity at height Z in the ABL (m/s)
W	width of the collector (m)
Z	height in ABL (m)
Z_G	gradient height in the ABL (m)

GREEK ALPHABETS

α	power law exponent
α_s	solar absorptance of the collector surface
ϵ	UTC plate heat exchange effectiveness
ϵ_f, ϵ_h, ϵ_b	heat exchange effectiveness at the front, hole and back of the plate respectively
η	UTC thermal efficiency
ν	kinematic viscosity of air (m^2/s)

ρ	density (kg/m^3)
σ	UTC porosity

ABBREVIATIONS

ABL	atmospheric boundary layer
BIPV/T	building-integrated photovoltaic/thermal
CFD	computational fluid dynamics
CHTC	convective heat transfer coefficient
JMSB	John Molson School of Business
UTC	unglazed transpired collector

CHAPTER 1

INTRODUCTION

1.1 *OVERVIEW*

Sustainability has gained immense importance over the past few decades. The Renewable Energy Policy Network for the 21st Century (REN21) reports that 16.7% of the world's final energy consumption is sourced by renewables, of which solar power constitutes only 5% (See Figure 1.1). Nevertheless, there has been commendable growth in the solar thermal industry in recent times – over 20% annually (NRCan, 2010).

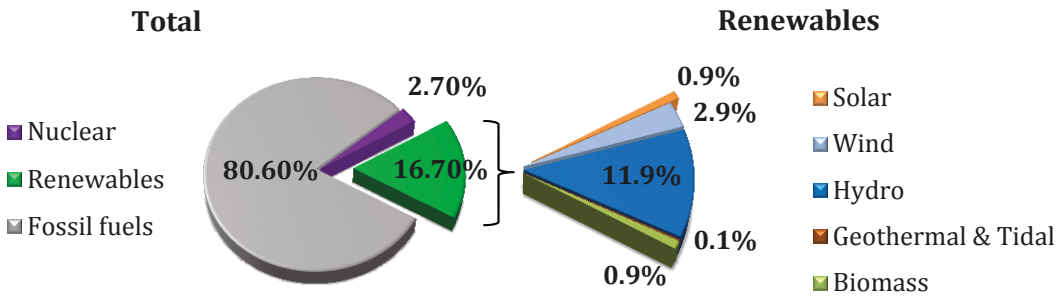

Figure 1.1: World Energy use by source (REN21, 2012)

This growth is partly attributed to improvements in the quality of technology that makes solar energy accessible, which in turn is a result of research and innovation on the contributive parameters; such is the study of the effect of wind on solar thermal collectors. High performance of solar thermal devices is brought about by reducing heat loss to a minimum. In this regard wind-induced convection heat loss is a major concern and extensive studies with wind simulations as accurate as possible are necessary to arrive at generalized guidelines for efficient system design.

1.2 *UNGLAZED TRANSPIRED COLLECTORS AND THE ROLE OF WIND*

Solar thermal collectors are composed of a dark absorber plate that absorbs solar heat and transfers it to a working fluid – typically water, air or in some cases special fluids such as glycol – which is then circulated in the system to be heated. An unglazed transpired collector (UTC) consists of a perforated (about 1% - 7% of the area) absorber cladding installed about 10 – 20 cm off the sun-facing wall of a building, forming a plenum behind the cladding. Figure 1.2 shows the schematic of a typical UTC. Heat absorbed by the metal cladding forms a layer of warm air on either side. Negative pressure is created in the plenum using a fan located behind the wall at the top, whereby outdoor air is drawn in through the perforated cladding. During this process, heat from the absorber is transferred to the air and the heated air is distributed into indoor spaces through a duct system.

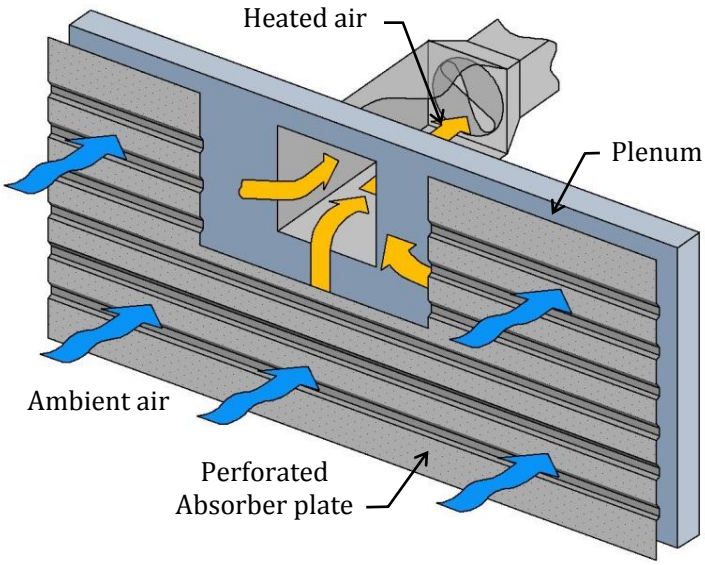

Figure 1.2: Schematic of a UTC

In addition to space heating, UTCs are known to be used for crop-drying in barns and heating swimming pools. The U. S. Department of Energy recognizes this technology as the most efficient air-heating system available today – 75% efficiency as claimed by Solarwall® (Heinrich, 2007). The most critical effect of wind on a UTC is forced convection heat loss. While winds normal to the collector could enhance the heat transfer effectiveness of the plate as the flow is in the same direction as the air being drawn in through the perforated absorber, high velocity winds flowing parallel to the collector's surface, could cause suction in the pores and thereby outflow from the plenum behind the collector. This results in the loss of useful heat being carried by the plenum air (Fleck et al., 2002) in addition to convective losses (Kutscher et al., 1993).

1.3 *BUILDING-INTEGRATED PHOTOVOLTAIC/THERMAL SYSTEM AT CONCORDIA UNIVERSITY*

The NSERC Smart Net Zero Energy Buildings Research Network (SNEBRN). SNEBRN is a collaboration of researchers from 15 Canadian universities, Natural Resources Canada (NRCan) and Hydro-Québec, dedicated to the facilitation of a widespread adoption of net-zero energy design concepts across the country. Under this initiative, the network designed and implemented a building-integrated photovoltaic thermal system (BIPV/T) that consists of a 288 m^2 UTC, overlaid with PV panels over a major portion of its area, integrated into the equator-facing façade of the John Molson School of Business (JMSB) building at Concordia University.

Figure 1.3: The John Molson School of Business building housing the building-integrated PV/thermal system

While PV panels produce electricity, ventilation air is preheated by heat from both the PV panels as well as the exposed UTC area. The performance of the BIPV/T system is continuously monitored and readings are fed to a data acquisition system; this includes plenum temperature, airflow characteristics, thermal and electrical production etc. In addition, the database also stores information from a rooftop weather station that records wind speed and direction, solar irradiance, temperature and humidity.

1.4 *RESEARCH OBJECTIVE*

The study presented in this thesis is in association with Theme II of the SNEBRN titled "Dynamic Building Envelope Systems and Passive Solar Concepts". One of the objectives of the theme is to study and optimize performance of building-integrated solar air-heating systems for facades and roofs including, but is not limited to, the consideration of wind effects. It is common practice in the analysis of UTCs to assume a wind velocity measured at a representative location, such as the roof of the building housing the UTC. However, wind does not impinge uniformly on all points on large areas. The velocity distribution depends on wind direction and surroundings of the concerned area; this could have an effect on the convective heat losses from UTCs and, in turn, its efficiency.

The present study is an attempt to demonstrate the significance of using actual velocity distributions corresponding to different wind directions, as opposed

to a single velocity value measured at a reference location, for UTC analyses. The impact of surrounding structures on the wind velocity distribution has also been studied. Using the solar system installation on the JMSB building as a base for reference full-scale measurements and experimental studies at the Building Aerodynamics Lab at Concordia University, the following steps were set forward to fulfill the objectives of this study:

- Experimental investigation of the wind velocity distribution for different wind directions on a vertical façade by wind tunnel studies
- Assessment of the impact of wind on a UTC and the error in assuming a uniform normal wind velocity distribution as opposed to using the actual uneven distribution in calculations of UTC performance parameters;
- Comparison of the results with a previous study done to assess wind effects on the SNEBRN solar-wall;
- Presentation of the practical implications of the results from this study.

1.5 *THESIS OUTLINE*

This thesis is structured into six chapters. Background knowledge on flow phenomena around buildings and its simulation in wind tunnels has been summarized in Chapter 2. A detailed review of past literature that contributed to the knowledge base needed to have completed this study is documented in Chapter 3. Details of the experimental equipment, full-scale data collection, selection of appropriate models and parameters for wind tunnel tests and sensitivity study and the experimental procedure are described in Chapter 4. Chapter 5 presents the results of the experiments, their interpretation and practical implications. The thesis concludes with Chapter 6 where the contributions of this study as well as recommendations for future work are discussed. A list of references is provided at the end.

CHAPTER 2

WIND ENGINEERING BACKGROUND

2.1 *WIND FLOW AROUND BUILDINGS*

Wind is highly stochastic in nature; it has a very dynamic and unsteady flow pattern because of which not every point on a plane in the path of flow has the same velocity. Wind has the highest velocity where the flow is not affected by any boundaries or obstructions, i.e. high elevations in the atmosphere. As the earth's surface is neared, wind is constantly under the effect of friction caused by ground level obstructions that retards the flow velocity. The degree of retarding depends on the terrain over which air flows and the height above the earth's surface under consideration. At any given height over fairly open terrains such as the sea or grasslands, wind velocities are higher than what would be experienced at the same height over a rougher terrain such as dense forests or city centers (Figure 2.1). The minimum height at which wind is no longer affected by ground obstructions is called gradient height (Z_G); this height represents the thickness of the atmospheric boundary layer. Above the atmospheric boundary layer, wind speed is assumed constant and is termed gradient wind speed (V_G). The wind speed at ground level is assumed to be zero and the variation of mean wind speed with height in the

atmospheric boundary layer is approximately represented by the well-known power law, expressed as:

$$\frac{V_Z}{V_G} = \left(\frac{Z}{Z_G}\right)^{\alpha} \tag{2-1}$$

where, V_Z is the mean wind velocity at any required height Z in the terrain represented by the power law exponent α. Table 2.1 shows values of V_G and α used to represent different terrains, as suggested in various codes and literature. In a particular city, the gradient wind speed is assumed to be the same in different terrains; the gradient height however varies (see Figure 2.1).

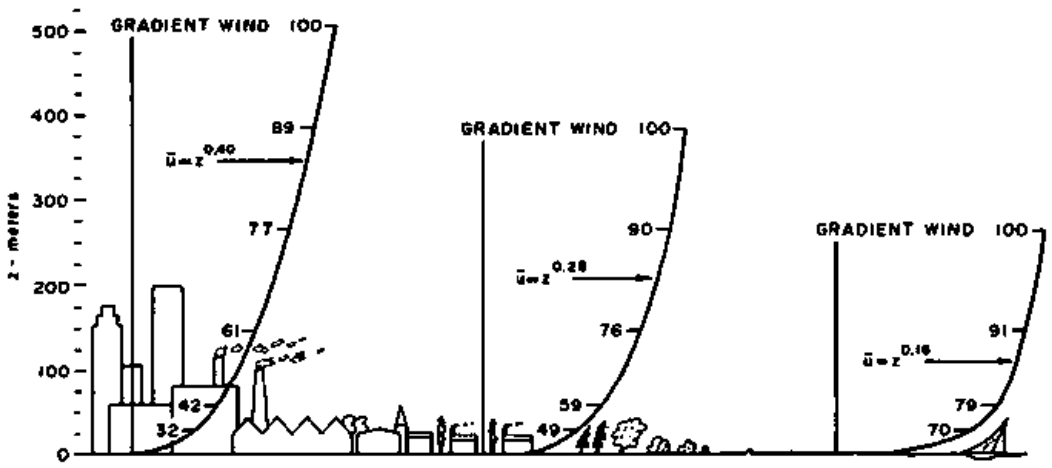

Figure 2.1: Profiles of mean wind velocity over level terrains of different roughness (Davenport, 1967)

Table 2.1: Gradient heights and power law exponents for different terrain types (Simiu, 1981; Holmes, 2007; Stathopoulos, 2007)

Terrain description	Gradient height Z_G (m)	Power law exponent α
Very flat terrain: *rough sea, snow, ice, desert*		0.10 – 0.12
Open terrain: *grasslands, scarce vegetation*	275	0.14 – 0.22
Suburban terrain: *low buildings*	400	0.25 – 0.30
Urban terrain: *heavily built up city centers*	500	0.30 – 1.40

In urban areas, the airflow is affected by additional unsteadiness associated with the aerodynamics of buildings. When wind impacts on a building, it tries to find the nearest exit path around, over or through the building; in this process, the flow accelerates around corners and edges, thereby inducing high suction at these surfaces. Consider the basic case of perpendicular wind approaching an isolated rectangular building; as shown in Figure 2.2, the building intercepts the wind, brings it to a rest at the 'stagnation point' and redirects it from its normal path. Air flows along the building surface until it reaches the edges where the flow 'separates' and continues to form a turbulent wake region behind the building or gets 'down-washed' towards ground-level. Above the 'stagnation point', the flow is typically in an upward direction up to the separation point. In the case of non-isolated or closely located buildings as in an urban setting, in addition to wind-structure interactions, local flows interact with each other thereby making flow patterns even more complex and cumbersome to evaluate analytically.

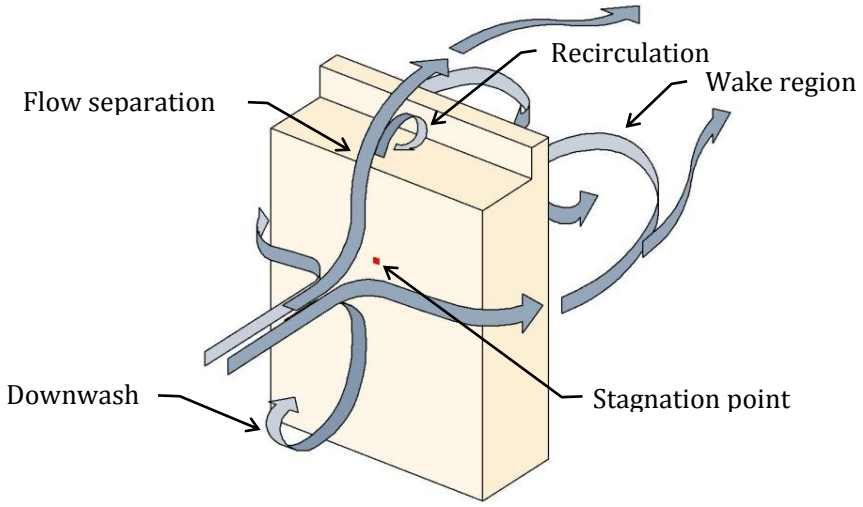

Figure 2.2: Air flow around an isolated building with perpendicular wind

The stagnation point and parallel flows may or may not occur in urban areas depending on the sheltering offered by the immediate surroundings of the building. Wind tunnel testing is the most robust and extensively used method to investigate the effects of such involute flows.

2.2 *BOUNDARY LAYER WIND TUNNELS*

A wind tunnel is used to simulate natural characteristics of wind and its interaction with man-made objects or structures at an appropriate scale. Although wind tunnels have been in existence for a very long time, and were used for aeronautical studies, it was only in recent decades that boundary layer wind tunnels were established and buildings and bridges were studied extensively. As the name

indicates, these wind tunnels simulate the atmospheric boundary layer by allowing wind to flow over a long fetch of roughness elements (this is not required for aeronautical studies that deal with wind flow above the boundary layer). Accurate simulation of the atmospheric boundary layer characteristics, such as the velocity profile, turbulence intensity and power spectra of turbulence, is attained by the appropriate choice of building model scales based on the dimensions of the wind tunnel, size of the building and objectives of the study. Figure 2.3 by Stathopoulos (1984) shows the comparison of the spectra of longitudinal turbulence measured in the boundary layer wind tunnel at Concordia University with analytical (Von Karman's) and empirical (Davenport's) representations of the spectra of natural wind. The similitude was observed to be satisfactory for a scale of 1:400.

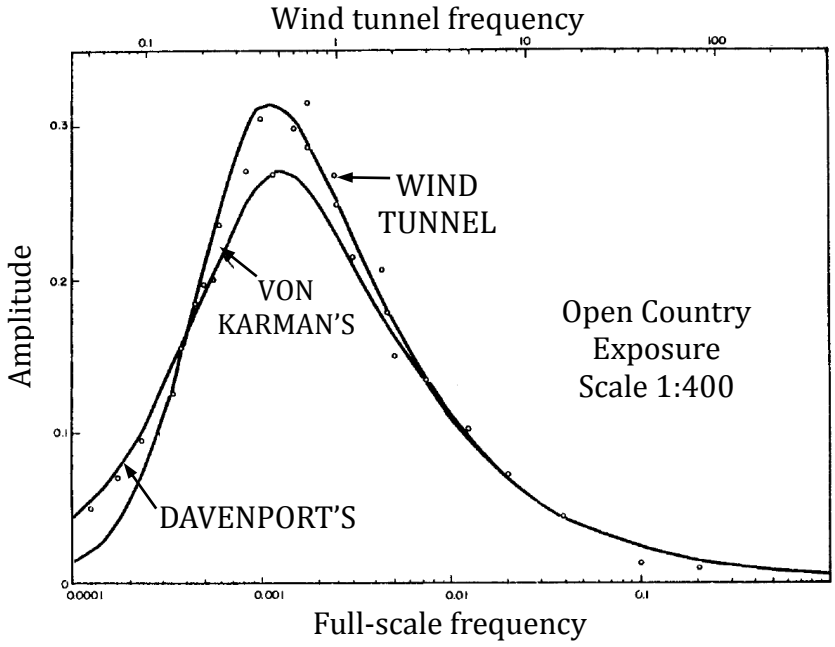

Figure 2.3: Longitudinal turbulence spectra of wind (Stathopoulos, 1984); modified

CHAPTER 3

LITERATURE REVIEW

3.1 *A BRIEF HISTORY OF SOLAR COLLECTORS*

Historical architectural records claim the use of solar energy for heating homes since the 1700s. The most traditional method of using solar energy in homes is the provision of large equator-facing fenestration by which natural light and heat were flushed into the interior spaces. Edward S. Morse has been accredited for the design and production of the first modern solar air heater in 1881 (Morse, 1881; Moore, 2005). Morse's design, seen in Figure 3.1, consisted of a simple assembly of a glass covered black sheet of metal that absorbed the sun's heat, attached to a timber cabinet hung on a wall with sufficient distance between the wall and metal for airflow; very similar to the Trombe wall which was introduced in the late 1980s. Cool air from the building entered the bottom of the cabinet in the space created by rising air – heated by the metal – that moved into the building. Although at the time the design received very little attention, Morse's design remains the basic framework for modern day solar collectors.

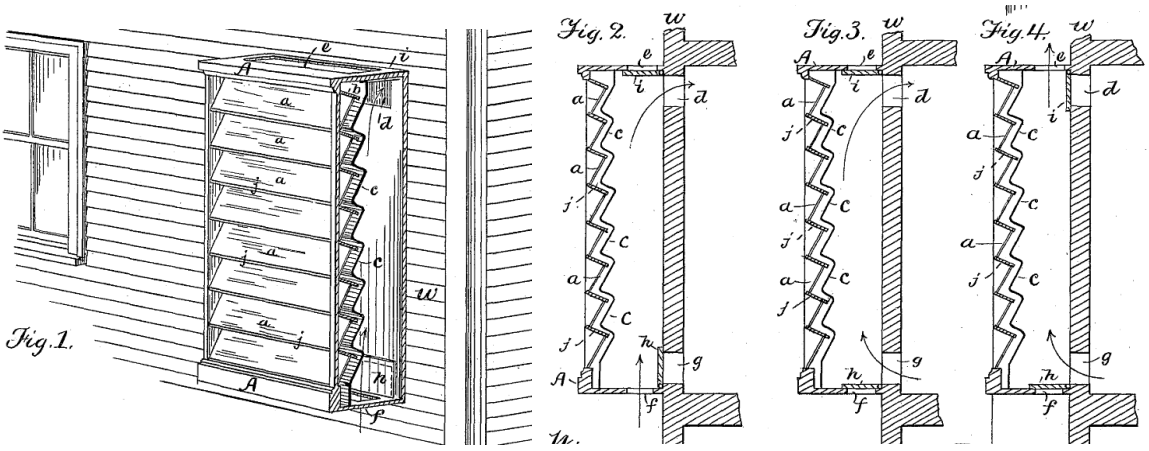

Figure 3.1: Schematic of the solar collector design by Morse (Morse, 1881)

The next level of developments in solar energy technology was the use of thermal mass for interior heating. The concept of thermal mass began to grab attention with the introduction of the House of Tomorrow in 1932 and the Crystal House in 1933, by architects G & W Keck at the Chicago World fair, where the masonry walls and floors played a major role in heating the house during winter. The late 1940s saw the introduction of phase change materials and advancements in traditional solar collectors. Powered by the energy crisis in the 1970s, there was an upsurge in funded research programs in the renewable energy field, especially solar devices. The following two decades saw commendable development in photovoltaic (PV) and thermal technology and their integration into building façades. The unglazed transpired collector (UTC), introduced in 1989 (NREL, 1998), is one of the most efficient solar collectors available today.

3.2 *WIND EFFECTS ON UNGLAZED TRANSPIRED COLLECTORS*

UTC performance is governed by a number of factors such as ambient temperature, wind speed, properties of the absorber plate, pitch and diameter of the perforations, air suction rate etc., most of which have been addressed in various past studies. Air exiting at the back of the plate, i.e. the outlet air, is at a lower temperature than the plate surface. The air heating effect of the plate, defined by the so-called heat exchange effectiveness of the absorber, has been shown to be an important factor in determining the UTC performance efficiency. A number of research studies have focused on establishing a function for heat exchange effectiveness. Some of these studies contributed useful information relevant to the present study and are summarized as follows:

- ***Kutscher (1992, 1994)***

One of the earliest studies by Kutscher in 1992 investigated heat transfer on low porosity plates, the results of which were meant to apply in UTC analysis. Theoretical examination of the different modes of heat loss from UTC, assuming laminar airflow parallel to the collector, yielded the following relations for convective heat loss Q_{conv} and collector efficiency η:

$$Q_{conv} = 0.82\left(\frac{V_\infty \nu}{V_s^2}\right) W\left[\rho c_p V_s (T_{coll} - T_{amb})\right] \tag{3-1}$$

$$\eta = \alpha_s \left[1 + \left(\frac{h_r}{\epsilon} + h_c\right)\left(\rho c_p V_s\right)^{-1}\right]^{-1} \quad (3\text{-}2)$$

where, V_∞ is the free stream wind velocity, V_s is the velocity with which air is drawn through the UTC perforations, T_{coll} and T_{amb} are temperatures of the collector surface and ambient air respectively and h_r and h_c are coefficients of heat transfer by radiation and convection respectively. Plate heat exchange effectiveness ϵ, relates the outlet air temperature T_{back}, plate surface temperature and ambient air temperature (Kutscher, 1992):

$$\epsilon = \frac{T_{back} - T_{amb}}{T_{coll} - T_{amb}} \quad (3\text{-}3)$$

It was found that radiation to the sky and ambient air affected UTC efficiency significantly. For suction velocities (V_s) greater than 0.05 m/s, the efficiency were found to be nearly constant and independent of wind speed. The study concluded that heat losses due to natural convection are negligible, and those due to wind should be small for large collectors operated at typical suction velocities. The explanation was that wind-induced convection occurred only over a 'starting length' where the boundary layers were growing (see Figure 3.2) beyond which the boundary layer was asymptotic, maintained by the uniform suction through the UTC plate. Kutscher showed analytically that for 10 m/s wind speed and 0.05 m/s suction velocity on a UTC at an average temperature of 30°C, the convective heat losses are equivalent to the net solar energy on a 5 cm wide strip of the collector

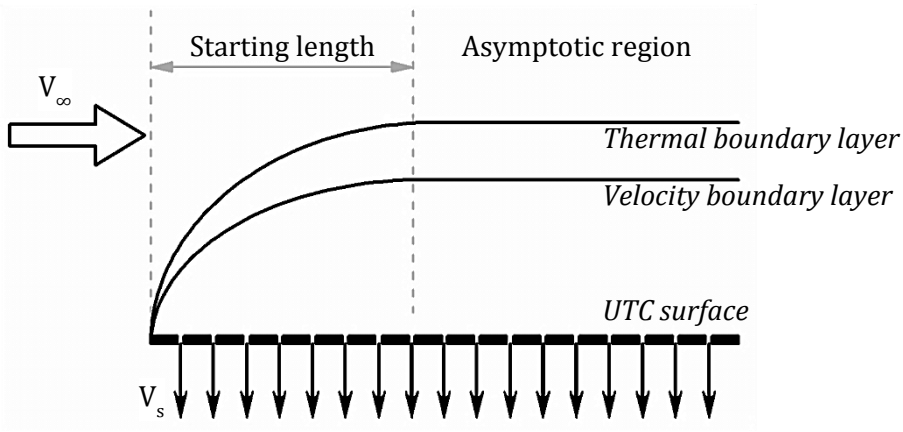

Figure 3.2: Development of thermal and velocity boundary layers over a UTC plate; recreated from Kutscher (1992)

which, on a large collector spanning several metres, is negligible. .Commenting on non-parallel flows, Kutscher stated that wind-induced convective heat loss would be greater than that estimated by equation (3-1) and that for large collectors, the formation of a stagnation point makes it *"…reasonable to assume that the local wind is in a direction parallel to the wall* (Kutscher, 1992, p. 38)".

The assumption of parallel laminar boundary layer in this study poses as a limitation to its application in UTC analysis. In reality, as explained in chapter 2 (Section 2.1), stagnation point and parallel flow conditions are characteristics of airflow around bluff bodies; however these phenomena are subject to conditions of open surroundings and unobstructed approach wind. The asymptotic boundary layer assumption also would hold true only for unidirectional airflow parallel to the collector's surface, which is seldom the case for actual airflow around buildings. Moreover, the boundary layer is not actually laminar as assumed by Kutscher

(1992), which means that convective heat transfer may not be limited to a small length of the UTC and therefore not a negligible quantity (Fleck et al., 2002).

Heat exchange effectiveness ϵ is a key parameter in UTC analyses as the thermal efficiency can be calculated easily if the value of ϵ is known. Kutscher's research was extended to an experimental analysis in a wind tunnel to assess the effect of crosswind on ϵ (Kutscher, 1994). A series of perforated plates with different perforation orientations and pitch (spacing) were tested and it was shown that ϵ was dependent on a number of factors such as flow rate, orientation of perforations and crosswind speed. The study concluded that higher ϵ values could be obtained if the perforations are oriented with narrower spacing along the crosswind direction.

- ***Dymond & Kutscher (1997)***

The aim of the computer simulation study by Dymond & Kutscher was to develop a program for UTC analysis that could run on a personal computer without the need for any sophisticated hardware additions and long computational time. This program would allow designers to run parametric analyses quickly to assess the effects of changes in UTC parameters on their designs.

The modeling algorithm was derived by applying a pipe network analogy to the plenum flow and simultaneously solving mass conservation and thermal energy balance equations for the flow network and finally plugging the model into a commercially available CFD code named TASCflow. Based on the results from the

model runs, the study concluded that the suction velocity in the perforations was highest near the plenum exit, i.e. the fan location, and is reduced dramatically at locations farther away from the plenum exit. Correspondingly, the absorber surface temperature was lowest at points of highest suction velocity – meaning that higher the air flow through the absorber, greater the heat transferred away and therefore higher the thermal efficiency of the absorber.

- ***Van Decker, Hollands & Brunger (2001)***

Van Decker et al. extended the work initiated by Kutcher (1994) and studied the heat exchange effectiveness for plates of various materials, thickness, pore size, pore shape and pitch. Nine test plates with different combinations of these parameters were tested in an experimental apparatus that consisted of a heat source, air suction system, wind tunnel and data acquisition system. Based on experimental measurements and analytical models available in previous literature, the study developed isothermal predictive models for heat exchange effectiveness at the front ϵ_f, holes ϵ_h and back ϵ_b of the collector plate and over-all heat exchange effectiveness ϵ was expressed as follows:

$$\epsilon = 1 - \left(1 - \epsilon_f\right)(1 - \epsilon_h)(1 - \epsilon_b) \tag{3-4}$$

$$\epsilon_f = \frac{1}{1 + Re_s \min\left[aRe_w^{-\frac{1}{2}}, f\right]} \tag{3-5}$$

$$\epsilon_h = 1 - \exp\left[-4\left(c\frac{P}{D} + \frac{3.66}{PrRe_h}\frac{t}{D}\right)\right] \tag{3-6}$$

$$\epsilon_b = \left(1 + eRe_b^{\frac{1}{3}}\right)^{-1} \tag{3-7}$$

where, Re is the Reynolds number, D and P are diameter and pitch of the UTC perforations. A detailed list of symbols used and their descriptions are provided in the Nomenclature section on page xii. It was predicted that, of the total heat transferred, about 62% occurred on the front surface, 28% in the hole and 10% at the back of the plate. Through experiments and global regression fits, the values of the constants in equations (3-5), (3-6) and (3-7) were found to be a=1.733, c=0.004738, e=0.2273, f=0.02136 and Pr=0.71 (for air). The study arrived at the following model for heat exchange effectiveness of a UTC (Van Decker, et al., 2001) that was stated to be suitable for cases with and without wind and accounted for the effects of a wide range of variables that were considered in the experiments.

$$\epsilon = \left[1 - \left(1 + Re_s\, max\left[1.733Re_w^{-\frac{1}{2}}, 0.02136\right]\right)^{-1}\right] \times \left[1 - \left(1 + 0.2273Re_b^{\frac{1}{2}}\right)^{-1}\right] \times \exp\left(-0.01895\frac{P}{D} - \frac{20.62}{Re_h}\frac{\mathrm{t}}{\mathrm{D}}\right) \tag{3-8}$$

- ***Fleck, Meier & Matović (2002)***

The objective of this study was to examine the effects of wind speed and direction on UTC performance. Field tests were conducted on a fully functional UTC mounted on a building; UTC airflow rate & temperature, wall surface temperature, solar irradiance, ambient conditions, reference wind speed at 10 m elevation and

local wind speed at 61 cm from the collector surface were monitored and analyzed. The results showed that turbulent fluctuations exist outside the boundary layer enhancing convective losses on the UTC surface. It was also shown that peak collector efficiency occurred at wind speeds between 1 and 2 m/s and not at zero wind conditions as postulated by Kutscher (1993). This was confirmed later by Cordeau & Barrington (2011) who also conducted field measurements on UTC for broiler barns and found a maximum efficiency of 65% for wind velocities below 2 m/s and efficiencies below 25% for wind velocities higher than 7 m/s. Fleck et al. (2002) stated that the relation between collector efficiency and wind direction, based on their results, was inconclusive due to the lack of sufficient data. The study addressed certain drawbacks in Kutscher's studies viz. the use of laminar uniform flow parallel to the ground, which in reality is not the case of flow around bluff bodies.

- ***Gunnewiek, Hollands & Brundrett (2002)***

Winds parallel to the collector's surface above certain velocities, depending on the air intake rate of the collector, causes suction in the pores and thereby outflow through the pores. This results in the loss of useful heat being carried by the plenum air (Fleck, et al., 2002). Gunnewiek et al. (2002), who examined wind effects on the flow distribution in the UTC plenum using CFD simulations, addressed the phenomenon of reverse flow from the plenum. The study confirmed that high wind speeds raise the required suction velocity to maintain inward flow in the absorber

and plenum. This effect is localized to a region on the wall just below the roof edge; this is one of the areas on a building façade that experiences high suctions because of separated flow and acceleration of wind over the building edge.

- ***Athienitis, Bambara, O'Neill & Faille (2010)***

Athienitis et al. (2010) designed and developed a prototype PV/thermal panel that consisted of a UTC system with 70% of its area covered by PV panels (O'Neill, et al., 2011). Ventilation air is preheated by heat from the PV and the uncovered UTC. The PV/T system was integrated into the façade of an institutional building in Montreal, Canada. The design and analysis of the system considered the effects of only parallel wind flow for a range of speeds less than 2 m/s (Athienitis, et al., 2010).

Predominant winds for the location of the building are normal to the building integrated photovoltaic/thermal (BIPV/T) wall, as opposed to parallel airflow commonly considered in many previous studies that dealt with heat loss from UTC. Wind effects on the performance of this UTC were examined by Vasan and Stathopoulos (2012) using wind tunnel experiments; preliminary results showed that wind direction does indeed have an impact on the convective heat losses and efficiency of UTC.

3.3 *CONVECTIVE HEAT TRANSFER COEFFICIENTS ON VERTICAL FAÇADES*

Numerous researchers in the past have studied through field measurements, experiments and numerical analyses, the convective heat transfer coefficients (CHTC) on horizontal and vertical flat plates, the first of which were mostly for aeronautical applications. Research on convective heat transfer in the context of building surfaces began much later in the 1960s. These studies were directed for applications related to building components such as glazing, walls and more recently façade-integrated thermal collectors.

One of the earliest reported CHTC-wind velocity relations for a vertical surface was developed by Jürges (1924) in a wind tunnel study that measured heat transfer from a vertical heated plate attached to the sidewall of the wind tunnel for a range of free stream wind tunnel velocities V_∞:

$$h_c = 4.0V_\infty + 5.6 \tag{3-9}$$

The CIBSE Guide Book A (2006) provides a similar expression:

$$h_c = 4V_{loc} + 4 \tag{3-10}$$

where V_{loc} has been defined as the velocity near the building surface without any mention of the co-ordinates of the measurement location such as distance from the building, height above the roof etc. This was the same definition provided as early as the 1979 edition of the CIBS Guide Book. In light of this, Sharples (1984) commented *"This lack of definition possibly explains how V which almost certainly represents a wind speed in a building surface boundary layer, has come to be substituted for Jürges'*

free stream wind speed V_∞*"* where '*V*' is the author's notation for V_{loc} defined in this thesis. In fact, many studies have shown that local velocity at the building surface is entirely different from free stream velocity. Moreover, small flat plates attached to the walls of a wind tunnel did not form the best representation for heat transfer from buildings under the influence of complex airflows; this led to the initiation of research studies on CHTC specifically for application to building surfaces.

Information that would contribute to the present research has more to do with wind-induced heat transfers on vertical surfaces in actual wind conditions. In order to get the best approximation of these effects it is most appropriate to look at the airflow near the building surface, which depends on wind direction and surrounding structures, rather than just free stream velocity. Notation for wind direction differs from study to study; therefore, for consistency this thesis follows the notation as illustrated in Figure 3.3.

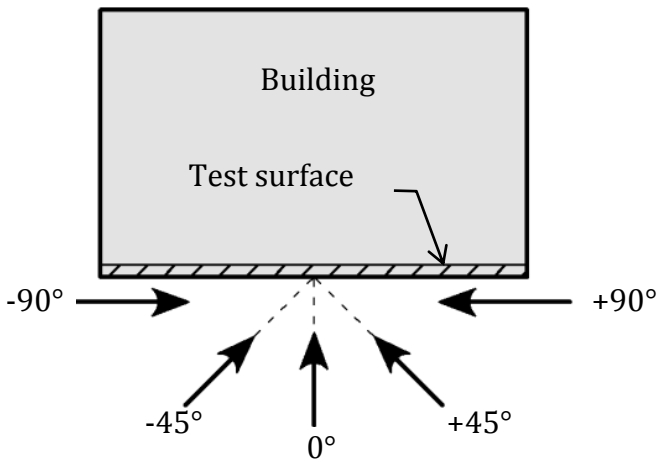

Figure 3.3: Illustration of the notation for wind directions

3.3.1 *Full-scale Studies*

The general methodology of full-scale studies to establish a relation between wind speed and CHTC at building surfaces involved the measurement of heat transfer from heated metal strips positioned high on the walls of tall buildings and wind velocity at primarily three locations – V_{ref} above the building roof, V_{10} at an elevation of 10 m usually at a nearby weather station and V_{loc} at a small distance, 0.3 to 2 m, from the test wall. Some of these studies relevant to the present study are discussed in this section.

- ***Ito et al. (1972)***

Ito et al. has been credited with one of the earliest and most significant works in the context of CHTC on building surfaces. Convective heat transfer from several locations on a six-storey building was measured at night so as to eliminate anomalies due to solar radiation. Local wind speed at 0.3 m from the building wall, reference wind speed 8 m above the roof and 10 m above ground at a nearby weather station were monitored and the following relations were obtained through data fits (Ito, et al., 1972):

$$V_{loc} = 0.25V_{10}\ ; \quad V_{10} > 2\ ms^{-1} \qquad \text{(3-11)}$$

$$V_{loc} = 0.5\ ; \quad V_{10} < 2\ ms^{-1} \qquad \text{(3-12)}$$

Windward surface

$$V_{loc} = 0.05V_{10} + 0.3 \qquad \text{Leeward surface} \qquad (3\text{-}13)$$

$$h_c = 18.6V_{loc}^{0.605} \qquad \text{All directions} \qquad (3\text{-}14)$$

where, h_c represents CHTC on the building wall. The main conclusions of the study were that V_{loc} values were 0.2 to 0.33 times the rooftop values for a windward surface when wind velocity is more than 2 m/s and that the full scale results were not in agreement with the CHTC values obtained using conventional relations if the velocity used in the formulas was the reference wind speed. CHTC-V_{loc} relationship was concluded to be independent of wind direction; however, it is not clear as to what wind directions data was collected for. The authors also stated that the ratio of V_{loc} to reference roof-top velocity increased with height at mid-width of the building and also towards the building edge for the 3rd and 4th floor of the six-storey building studied; it would have been beneficial to see the results for the top floor where the wind speeds would have been higher due to flow around sharp building corners. The shape of the building studied – which was an obtuse V-shape – also poses as a limitation to the generalized application of the expressions provided.

- ***Sharples (1984)***

In a study similar to Ito et al. (1972), Sharples (1984) made measurements of forced CHTC on a 78 m tall building located in an urban city center. Measurements were taken at several façade positions and their relationships with V_{loc} at 1 m from

the wall, V_{ref} at 6 m above roof level and V_{10} at a nearby airport were expressed as follows (Sharples, 1984):

$$V_{loc} = 1.8V_{10} + 0.2 \qquad \text{Windward surface} \qquad (3\text{-}15)$$

$$V_{loc} = 0.2V_{10} + 1.7 \qquad \text{Leeward surface} \qquad (3\text{-}16)$$

$$h_c = 1.7V_{loc} + 5.1 \qquad \text{All directions} \qquad (3\text{-}17)$$

Although the measurements were made at the top of a tall building, the study classified the wind directions as windward and leeward only, as done by Ito et al. (1972).

- ***Loveday & Taki (1996)***

This study involved full-scale measurements on the windward wall of an eight-storey rectangular building situated in a terrain the authors termed as 'semi-urban'. Wind speed and direction were measured at locations 11 m above the roof and 1 m from the external building surface that was being monitored.

It was found that when there is no wind, radiation is the predominant heat transfer mode; as wind speed increases, forced convection also gradually increases to become the dominant mode of heat transfer. In classifying wind directions, Loveday and Taki (1996) took an additional step and separated the data for wake flows that were defined as results of wind approaching from 70° to 90°. The

following relations were obtained based on linear regression fits on the data collected (Loveday & Taki, 1996):

$$V_{loc} = 0.68V_{ref} - 0.5 \qquad \text{Windward surface} \qquad (3\text{-}18)$$

$$V_{loc} = 0.2V_{ref} - 0.1 \qquad \text{Surface under wake flows} \qquad (3\text{-}19)$$

$$V_{loc} = 0.157V_{ref} - 0.027 \qquad \text{Leeward surface} \qquad (3\text{-}20)$$

$$h_c = 16.25V_{loc}^{0.503} \qquad \text{All directions} \qquad (3\text{-}21)$$

These relations were reported to have compared well to those in the previously cited studies. Although the study broadly classified wind directions as windward, leeward and wake flows only, it was shown that the highest CHTC values occurred for wind directions between 10° and 25° (see Figure 3.3 for wind directionality notation). The results presented are indeed very detailed however; the test plate was located at mid-width on the wall of the 6th storey of an eight-storey building. It is known that wind accelerates and hence separates at building edges and corners; therefore the $h_c - V_{loc}$ correlations could be different and h_c could be higher at these areas than what would have been predicted by correlations based on measurements at a central location.

❖ ***Liu & Harris (2007)***

This source presents a very detailed full-scale study on a single-storey test building located in open terrain. Apart from wind speed measurements – local wind speed at multiple locations 0.5 m off the test wall using an ultrasonic anemometer, reference wind speeds at 1 m above the roof using a three-cup anemometer and wind-vane and 10 m above the ground level by a local weather-station – local meteorological parameters such as solar radiation and humidity were also monitored; day-time measurements were separated from nocturnal measurements for analysis. Approach wind direction was shown to have a significant effect on wind-induced CHTC. The study presented separate equations relating CHTC to V_{loc} 30° wind direction segments, as shown in Figure 3.4, which represent wind-induced CHTC better than the broad classification as windward and leeward only that had been the norm in previous studies. Moreover, categorizing data into groups reduces the scatter in plots of CHTC versus velocity and allows for better regression fits. The following are selected equations from the study that are of relevance to the thesis; as an exception the original directionality notation used in the source has been followed here owing to the degree of detail in the results presented:

$$h_c = 5.90V_{loc} + 3.95 \qquad 75° \text{ to } 105° \tag{3-22}$$

$$h_c = 6.42V_{loc} + 3.17 \qquad 135° \text{ to } 165° \tag{3-23}$$

$$h_c = 7.42V_{loc} + 2.98 \qquad 165 \text{ to } 180° \tag{3-24}$$

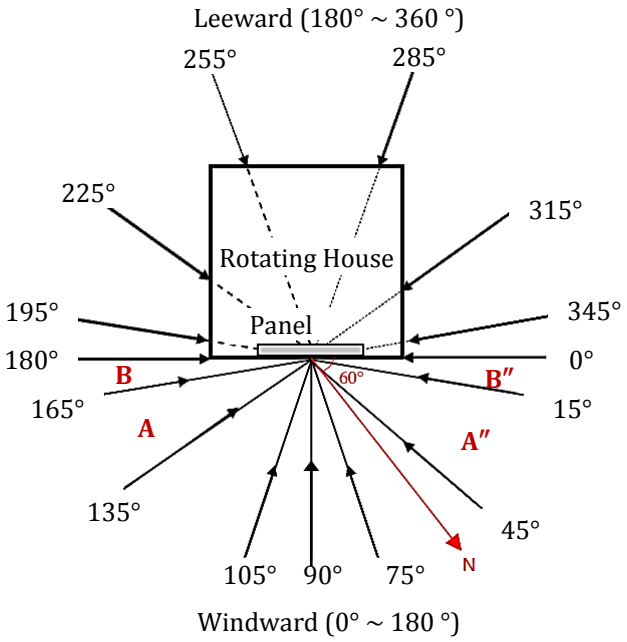

Figure 3.4: Illustration of the wind direction notation by Liu & Harris (2007); modified

It was stated that the slope of the regression lines increased with wind incidence angle on the building surface; it is evident from the results presented that this is due to the different sizes of data sets for the different wind speeds and directions. Had the data sets been of the same size and unbiased in terms of wind direction & wind speed, for a symmetrical building, the correlations for any two directions symmetrical about the normal to a wall (e.g. 0° & 180°, 15° & 165° etc. in Figure 3.4) would be expected to be the same. Equations (3-23) and (3-24), for segments A and B respectively, were developed from data sets that were larger than those for the respective symmetrically opposite directionality segments A″ and B″.

❖ ***Shao et al. (2010)***

The previously cited works were based on principles of heat balance on a test specimen. Shao et al. made use of the naphthalene sublimation method, which uses heat and mass transfer principles to calculate CHTC, by monitoring the sublimation rate of naphthalene due to wind at regular intervals. The measurements were done at a height of 17.3 m on two 25 m tall buildings on a university campus. Reference wind velocity was measured at 2.5 m above the roof and local wind velocity at 1 m from the test wall. The following equation was obtained for the relation between CHTC and local wind speed in all directions (Shao, et al., 2010):

$$h_c = 4.21V_{loc} + 6.01 \tag{3-25}$$

The results did not compare well to those of previous studies; the authors speculated that the discrepancy was due to differences in topography and dimensions of the walls used for the tests.

3.3.2 *Computational Studies*

The most recent works are primarily computational analyses focused on improving the accuracy of CHTC-wind velocity relations.

- ***Blocken et al. (2009)***

Blocken et al. (2009) performed CFD simulations of forced convective heat transfer on a 10 m tall cubic building for V_{loc} at 0.3 m and 1 m from the façade and V_{ref} of 3 m/s at building height. Several wind directions ranging from 0° to 90° were accounted for and CHTC-V_{loc} correlations of the following form were developed for the windward façade:

$$h_c = 10.2V_{loc}^{0.93} \qquad 0° \tag{3-26}$$

$$h_c = 9.2V_{loc}^{0.82} \qquad 45° \tag{3-27}$$

$$h_c = 7.7V_{loc}^{0.77} \qquad 90° \tag{3-28}$$

The study confirmed the influence of wind on heat loss from the windward façade as in the case of previously cited studies; however, relatively low variations of CHTC distribution on this façade was found for wind directions in the range of 0° to 67.5°, 0° being normal to the façade.

❖ ***Defraeye, Blocken & Carmeliet (2010, 2011)***

CFD studies by Defraeye et al. (2010) used similar configurations as Blocken et al. (2009). The surface-averaged CHTC over the windward face of a 10 m tall cubic building was reported as a function of V_{10}. Based on the study, a methodology for estimating the statistical-mean CHTC for building surfaces was proposed. This methodology and the results presented were stated to be "*...only valid for the windward and leeward surfaces of an isolated cubic body in a neutral ABL for an incidence angle of 0° at high Reynolds and low Richardson numbers, or comparable configurations*" (Defraeye, et al., 2011, p. 519).

3.4 *DISCUSSION*

The works cited in sections 3.2 and 3.3 were chosen based on their relevance to the present study. Previous studies have shown that wind direction is an important factor that determines heat losses from a vertical surface subjected to air flow. When the surface considered is a UTC, these losses are translated into reductions in the thermal efficiency of the collector. It is worth mentioning that a number of previous studies were based on measurements taken in open terrain conditions, i.e. with little or no obstruction to the approach wind flow, which is seldom the case in actuality. To the best of the author's knowledge, there have been

no comprehensive findings relating the approach direction of the wind to UTC performance.

Figure 3.5 shows the comparison between CHTC-V_{loc} relations for 0° wind direction (windward surfaces) from the studies cited in this chapter. Although there is a common trend in the variation of CHTC with wind speed, clearly, the results from each of these past works are widely separated from each other. The present study involves the application of experimental data into pre-established relations for UTC performance parameters, namely heat transfer effectiveness, thermal efficiency and CHTC. In order for this, it was necessary to adopt correlations that were developed for configurations similar to that used in the present study.

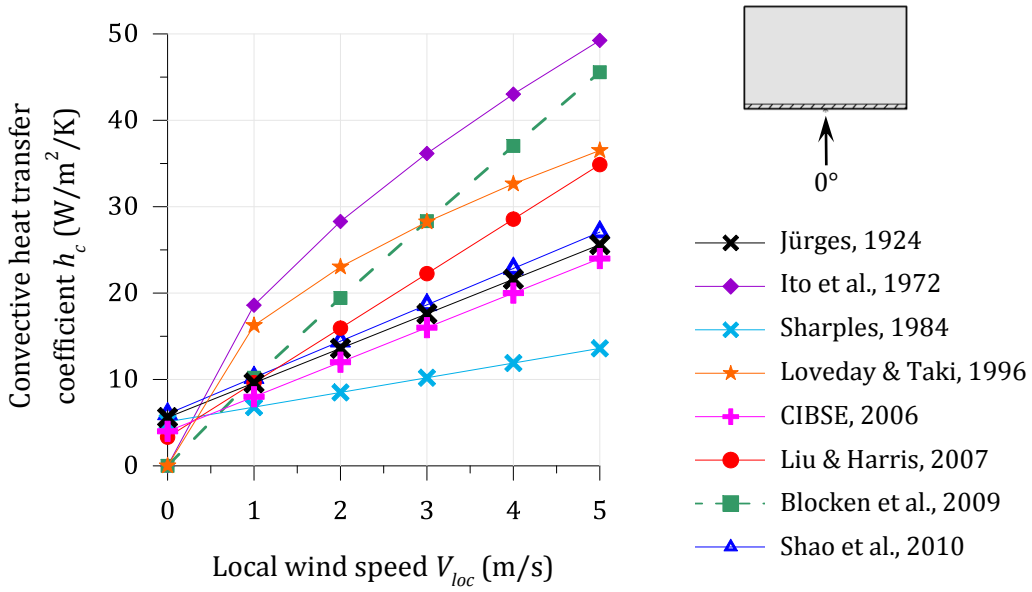

Figure 3.5: Comparison of CHTC-V$_{loc}$ correlations from cited works for 0° wind

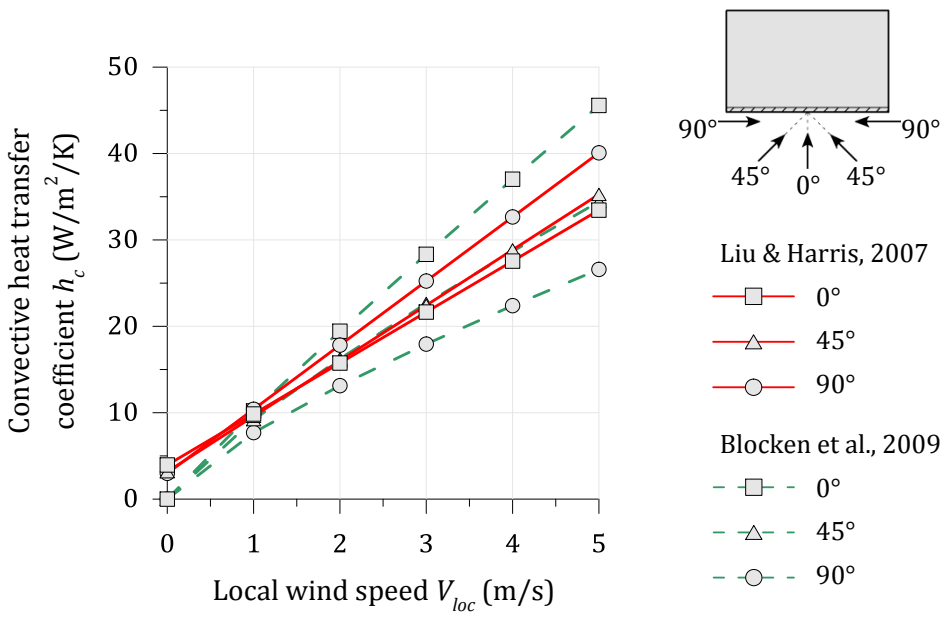

Figure 3.6: Comparison of direction specific CHTC-V$_{loc}$ correlations from Liu & Harris (2007) and Blocken (2009)

Liu & Harris (2007) and Blocken (2009) provide direction specific CHTC-V_{loc} relations; these have been compared in Figure 3.6. It can be seen that the difference between the directional plots are greater for Blocken's CFD correlations than the full-scale correlations by Liu & Harris. It is known and has been confirmed in literature (Sharples, 1984; Shao, et al., 2010) that natural convection losses are prevalent at zero wind speeds. This is not reflected in the power relations provided by Blocken (2009). The relations by Liu & Harris (2007) generate results that lie in between the range over which the results of other studies vary. Moreover, these relations were the most detailed and specific to different categories of wind directions which made it more accurate than a generalized equation for a broad range of wind directions. For these reasons, the CHTC-V_{loc} relations presented by Liu & Harris (2007) were considered apt for the present study.

CHAPTER 4

EXPERIMENTS

Preliminary steps in this study involved the retrieval of full-scale measurements of wind, solar and BIPV/T performance data from the JMSB database. The experimental study involved testing a small-scale model of the JMSB building in the Building Aerodynamics Laboratory at Concordia University for different wind directions and surrounding configurations. Details of the equipment, study model and procedure are presented in this section.

4.1 *JOHN MOLSON SCHOOL OF BUSINESS BUILDING*

The John Molson School of Business (JMSB) building, located in downtown Montreal, is 54 m tall. The solar system, integrated into the South wall, is 32 m long and 8 m wide extending from an elevation of 46 m to 54 m. The building houses a roof top weather station that provides solar irradiance and wind velocity data. The weather station anemometer is mounted on a 2.5 m tall mast situated 2 m away from the edge of the roof Figure 4.1 shows the location and orientation of the solar-wall and the anemometer. A large 3.5 m tall wall behind the anemometer shields it from winds approaching from the North, Northeast and East.

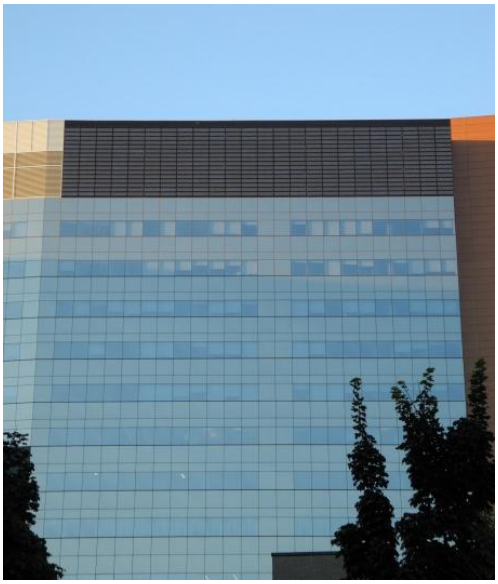

(a)

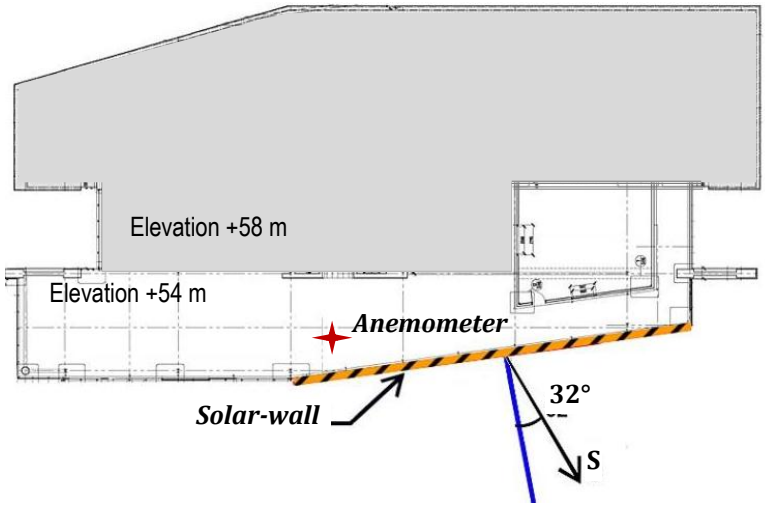

(b)

Figure 4.1: (a) Solar-wall on the JMSB building;
(b) Schematic plan of the JMSB showing orientation and location of the solar-wall

4.2 *FULL-SCALE WIND VELOCITY DATA*

The JMSB building houses a windmill type anemometer consisting of a propeller and a vane, shown in Figure 4.2, mounted on a 2.5 m mast. Rotation of the propeller produces voltage signals proportional to the wind speed. A potentiometer calibrated for a constant voltage corresponding to an azimuth angle of 0° (North) is present in the instrument. Any difference in this voltage brought about by the rotation of the anemometer vane is sensed and recorded. Based on the calibration of the instrument, the voltage signals resulting from the rotation of the propeller and the vane are converted to wind speed in m/s (accurate to ±0.3 m/s) and direction angle in degrees measured clockwise from North (accurate to ±3°).

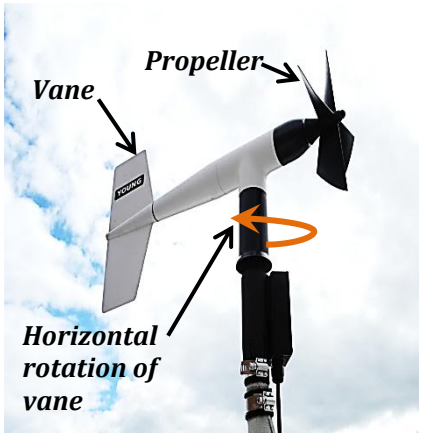

Figure 4.2: Anemometer at the JMSB weather station

All measurements taken by the rooftop weather station are archived in the JMSB BIPV/T system database. The hourly average wind speed and direction for every day from April 1, 2011 to March 31, 2012 were retrieved from the database. This range of dates was chosen because a continuous set of readings was available for this period. For the same period, hourly averaged data collected by Environment Canada at the Montreal-Pierre Elliott Trudeau International Airport was obtained from the website of the National Climate Data and Information Archive (Environment Canada, 2012).

4.3 *WIND TUNNEL EQUIPMENT AND EXPERIMENTAL SET-UP*

4.3.1 *Boundary Layer Wind Tunnel*

The Building Aerodynamics laboratory, located in the Engineering complex at Concordia University, houses an open circuit wind tunnel that is 12.2 m in length and 1.8 m in width with a suspended roof that allows the height to be adjusted between 1.4 m and 1.8 m. The wind tunnel can be operated at velocities from 3 m/s to 14 m/s. A turntable, of diameter 1.6 m, at the test section allows the model to be rotated to account for different wind directions. A honeycomb mesh and flow conditioning spires placed in front of the centrifugal blower "straighten" the flow by removing turbulence created by the fan. Figure 4.3 shows a schematic of the wind tunnel, construction details of which were presented by Stathopoulos (1984).

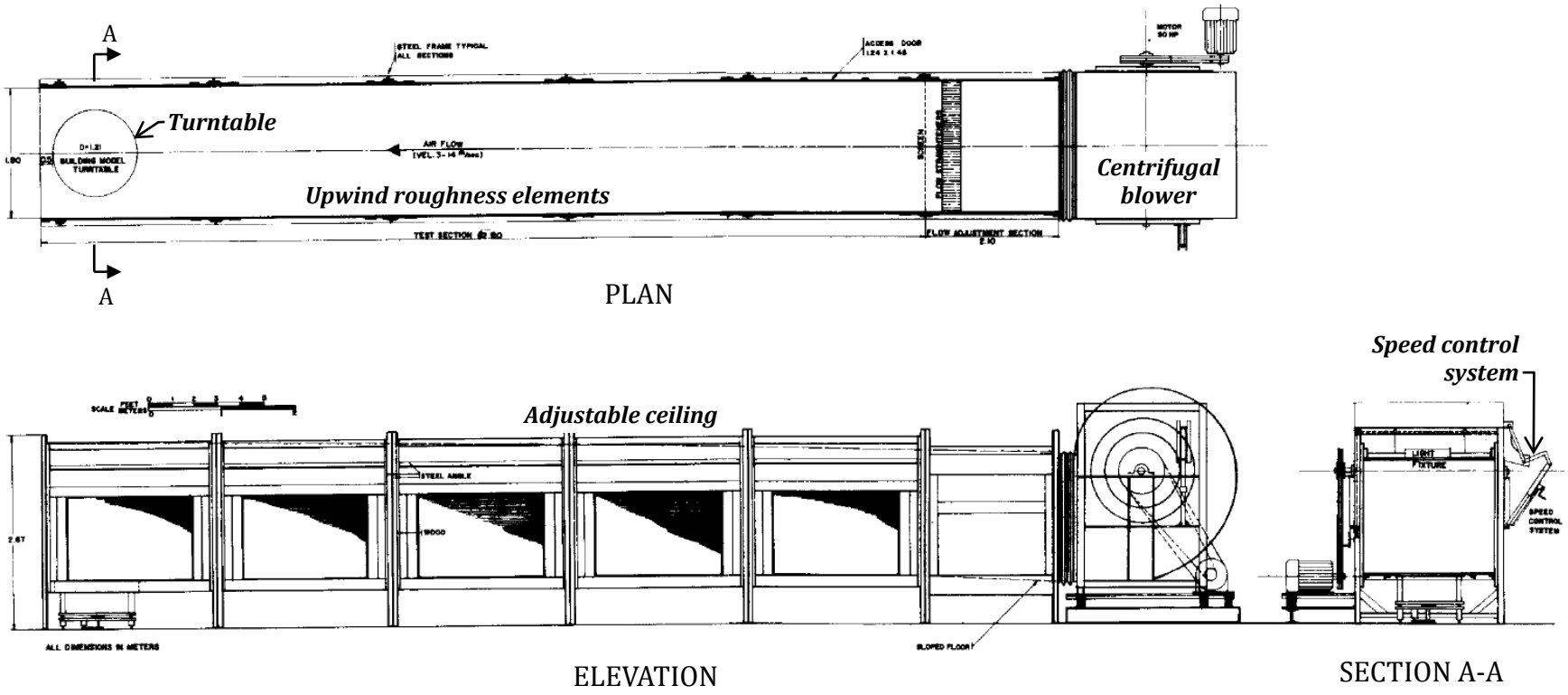

Figure 4.3: Schematic of the boundary layer wind tunnel at Concordia University (Stathopoulos, 1984); modified

4.3.2 *Study model and surroundings*

The JMSB building is surrounded by several buildings of similar height. As discussed in section 2.1, this affects the local wind flow and therefore, has been accounted for in this study. After the design and construction of the boundary layer wind tunnel, Stathopoulos (1984) established that a model scale of 1:400 was most appropriate for obtaining the best results based on the wind tunnel dimensions and flow characteristics. This finding along with knowledge of the Concordia University neighborhood and the dimension of the turntable led to the decision that all surroundings within a full-scale diameter of 500 m, as shown in Figure 4.4, would be included in the study.

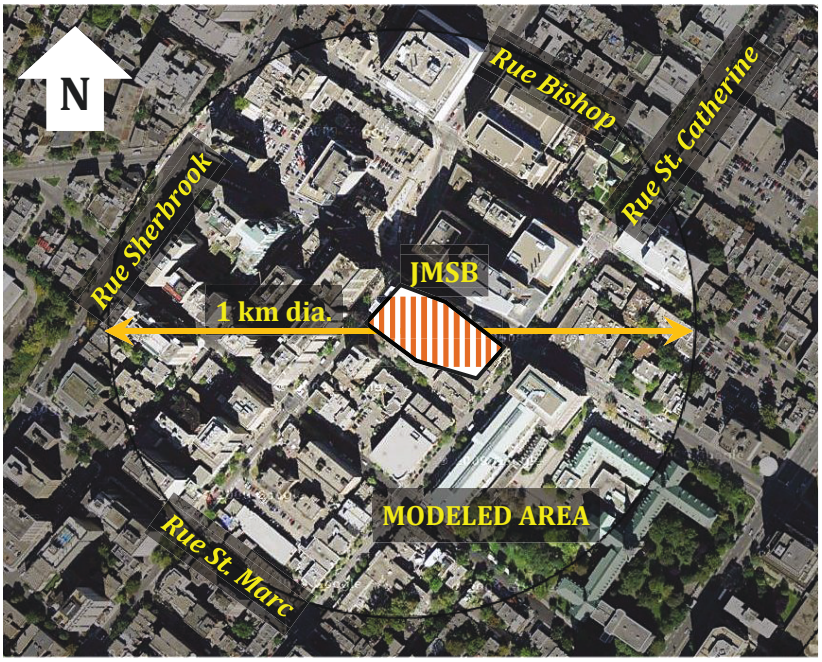

Figure 4.4: Aerial view of downtown Montreal showing the JMSB building and surrounding area that has been modeled

Simulation of the influence of the terrain beyond the modeled area is described in the following sections. Wooden models of the JMSB building and surroundings were constructed in 1:400 scale. The JMSB building model has a height of 13.5 cm and the area representing the solar-wall, hereafter referred to as 'test area', is 8 cm in length and 2 cm in height. These details have been illustrated in Figure 4.5.

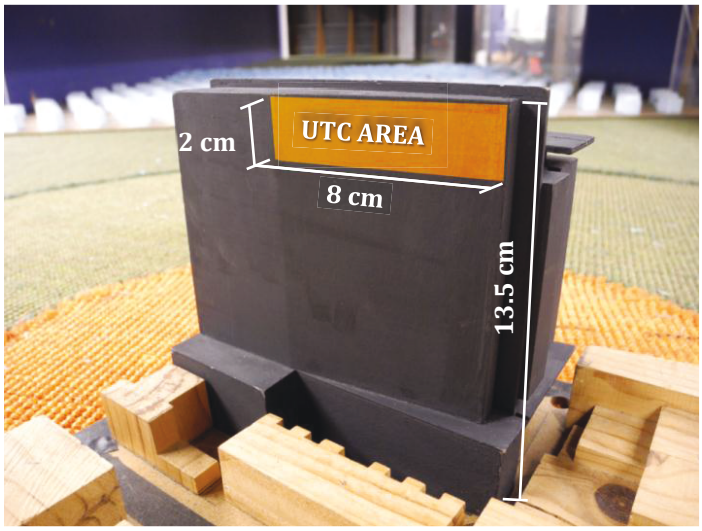

Figure 4.5: Test area on the JMSB building model at 1:400 scale

4.3.3 *Cobra Probe and 3-Dimensional Traversing system*

The 4-hole Cobra probe, from Turbulent Flow Instrumentation (TFI), is a flow measurement device that measures static-pressure and velocity and resolves the velocity components in real-time. It is about 16 cm in length and 1.4 cm in diameter, with a 5 cm long stem and 0.5 cm long head as shown in Figure 4.6.

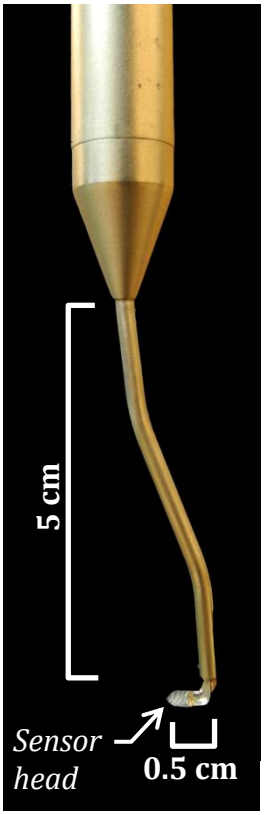

Figure 4.6: Cobra probe used for velocity measurements

Graphical user interface and data acquisition software of the instrument enable the control of the measurement process and display of the data on a computer screen in real time. The software stores this data in text files that can easily be imported into a spreadsheet program, like Microsoft Excel, for analysis.

A three-dimensional traverse system attached to the wind tunnel ceiling above the test section enables accurate positioning of velocity measurement devices at points of interest on the model. During the wind tunnel tests, the Cobra probe is mounted onto the 3-D traversing arm and positioned on the model using a control system whereby Cartesian co-ordinates of the point of interest are entered.

4.3.4 *Velocity Profile Simulation*

Since wind tunnel tests are done on reduced-scale models of buildings, in order to replicate the wind conditions the actual building experiences, simulation of the velocity profile and boundary layer holds immense importance. For this study, an urban wind profile was to be simulated. The required velocity profile and boundary layer thickness are simulated by passing the air over a long fetch of roughness elements – wooden panels affixed with egg-boxes (B) and Styrofoam cubes (A) – on the wind tunnel floor between the fan and the test section as shown in Figure 4.7. The choice and placement of roughness elements was verified by taking measurements of velocity V_Z at the center of the test section for different heights before placing the models. The plot of height Z versus wind velocity V_Z showed good agreement with the theoretical plot of velocity obtained using the power law for α = 0.3 and gradient mean velocity V_G= 12.7 m/s. As can be seen in Figure 4.8 the agreement is especially good at the region of interest from 10 cm to 15 cm in height. Thus, it was confirmed that profile developed had a power law exponent of 0.3 at the test section, which replicates the downtown terrain in Montreal to sufficient accuracy.

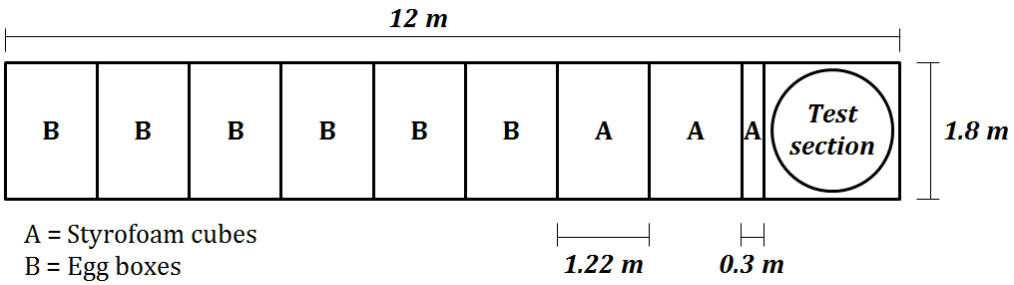

Figure 4.7: Roughness panel configuration in the wind tunnel for urban wind profile

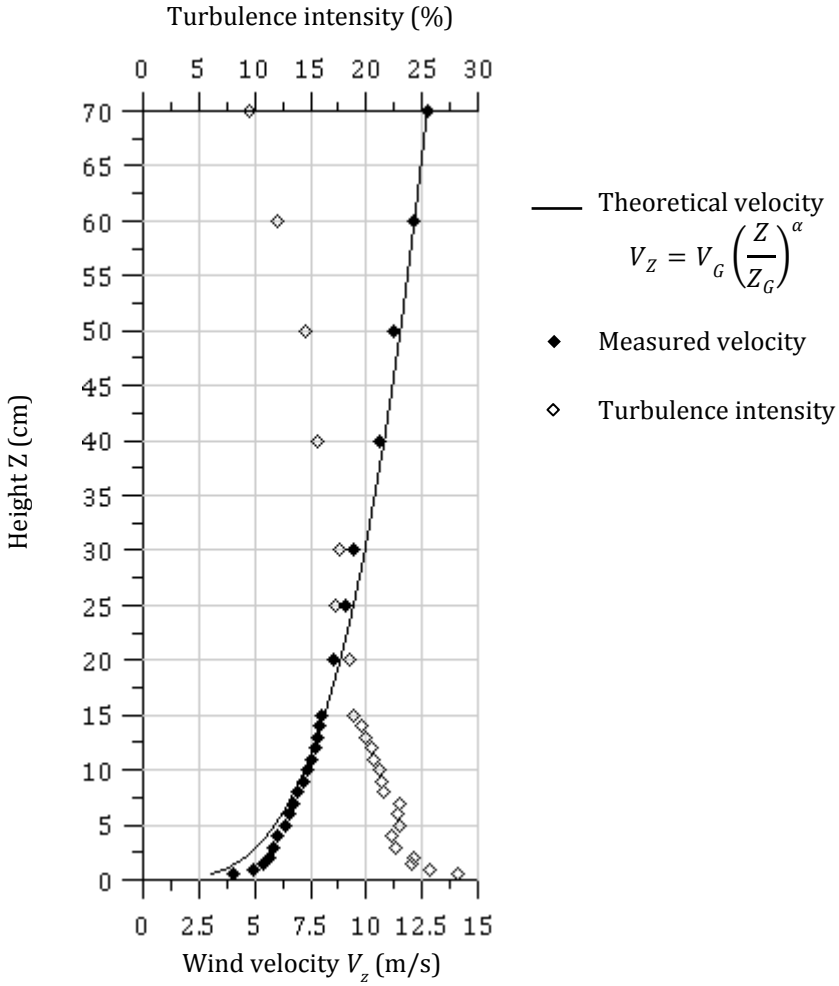

Figure 4.8: Comparison of wind tunnel velocity profile with the power law profile for α = 0.3 and scale 1:400

4.4 *WIND TUNNEL TEST PROCEDURE*

Based on the building's geometry and location in Montreal three wind directions, detailed in Table 4.1 and illustrated in Figure 4.9, were studied. Wind direction in this study is defined as the direction from which wind blows, measured counter-clockwise (+) or clockwise (-) from the normal to the test area (refer to Figure 3.2).

Table 4.1: Wind incidence angles used for experiments

Descriptor	Direction relative to the solar-wall	Cardinal direction
0° wind	Perpendicular	S32°W
45° wind	Oblique at 45° to the wall	S13°E
90° wind	Parallel	N52°W

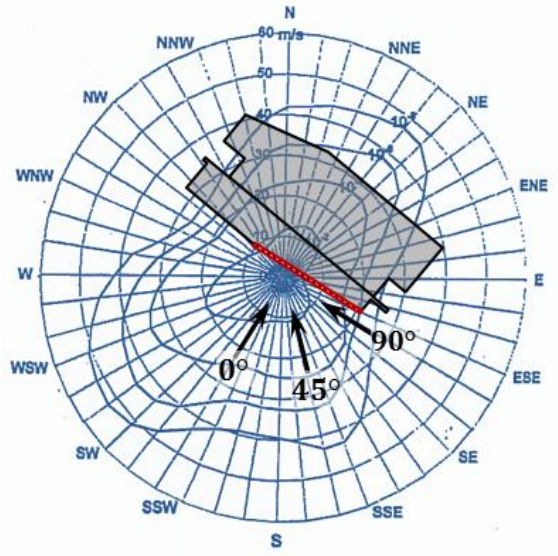

Figure 4.9: Wind-rose for Montreal overlaid with the JMSB plan showing the test wind directions and their incidence angles on the solar-wall

For the first round of wind tunnel tests, the models were placed on the turntable and oriented such that the solar-wall location, hereafter referred to as 'test area', was perpendicular to the free stream approach wind direction (0° wind). The Cobra probe was zeroed to remove any offset voltages before the wind tunnel was switched on. The wind tunnel was then operated at a speed of 12 m/s and the flow was allowed to stabilize. The Cobra probe was then placed in front of the test area by means of the traversing system and local velocity V_{loc} was measured at 40 points in an 8×5 grid pattern over the entire test area as shown in Figure 4.10. In addition, the reference velocity V_{ref} at a height of 6.25 mm above the roof of the model, hereafter referred to as the reference height, was also measured. This height, corresponding to 2.5 m above the roof in full scale, is the location of the anemometer that provided the full-scale reference wind-speeds. Each velocity reading was done for 30 seconds at a sampling frequency of 1000 Hz.

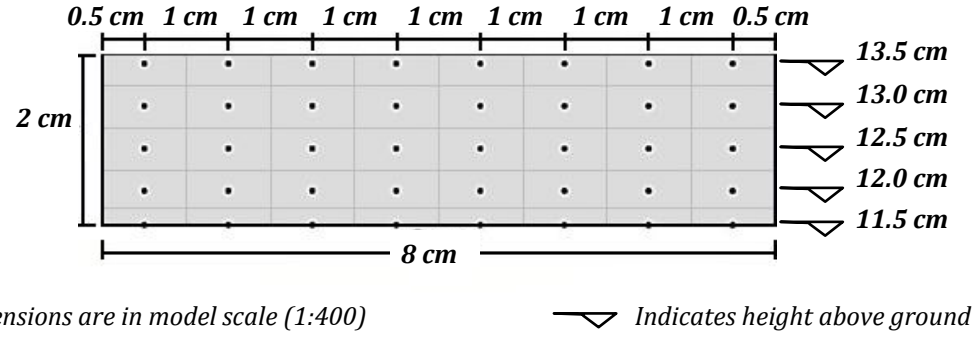

Figure 4.10: Schematic of the test area showing velocity measurement points

When the measurement for all locations was complete the wind tunnel was switched off, the turntable with the model setup was rotated so that the test area was positioned at 45° to the wind direction. The Cobra probe was zeroed and the procedure described above was iterated; the same was done for 90° angle as well.

The study also aimed to understand the impact of surrounding buildings on the UTC. In order for this, the above said procedure was carried out for two proximity model cases:

- Case 1: Test building with all existing surroundings (Figure 4.11a)
- Case 2: Test building in the absence of immediate surroundings (Figure 4.11b)

(a) **(b)**

Figure 4.11: Test wind direction - 45°
(a) Case 1: Test building with all existing surroundings
(b) Case 2: Test building in the absence of immediate surroundings

4.5 *SOLAR SIMULATOR EXPERIMENT*

The JMSB solar-wall studied in this was the subject of an experimental study in the solar simulator-environmental chamber laboratory (SSEL) at Concordia University (Bambara, 2012). The solar simulator is an indoor testing facility that reproduces natural sunlight and allows for testing of solar systems in controlled laboratory environments. It consists of a uniaxial platform on which the test subject is to be mounted and a light-source that emulates natural sunlight and an artificial sky that removes infrared heat from lamps (Figure 4.12a).

Solar simulator tests were conducted on a 1.50 m ×1.75 m test panel, similar to the JMSB solar-wall, mounted on the test platform in vertical orientation (see Figure 4.12b). The experimental setup included a fan, fixed below and about 10 cm in front of the test panel, that was used to blow a jet of air parallel to the test panel in a vertical, upward direction. The wind speed was measured using a hot-wire anemometer located 50 mm away from the surface of the UTC test panel. Ambient temperature was maintained at 20°C and measurements of outlet air temperature, air collection rate and pressure drop across the plenum were done for wind speeds of 1 and 3 m/s representing high and low wind conditions respectively.

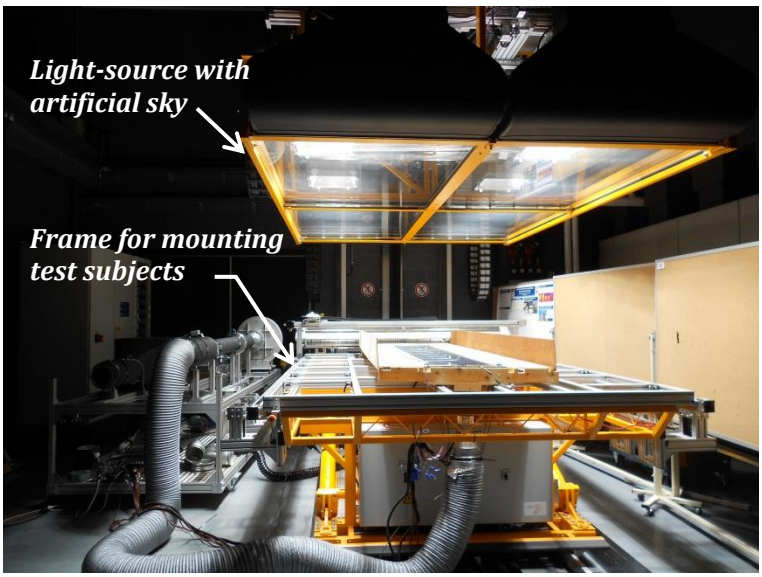

(a)

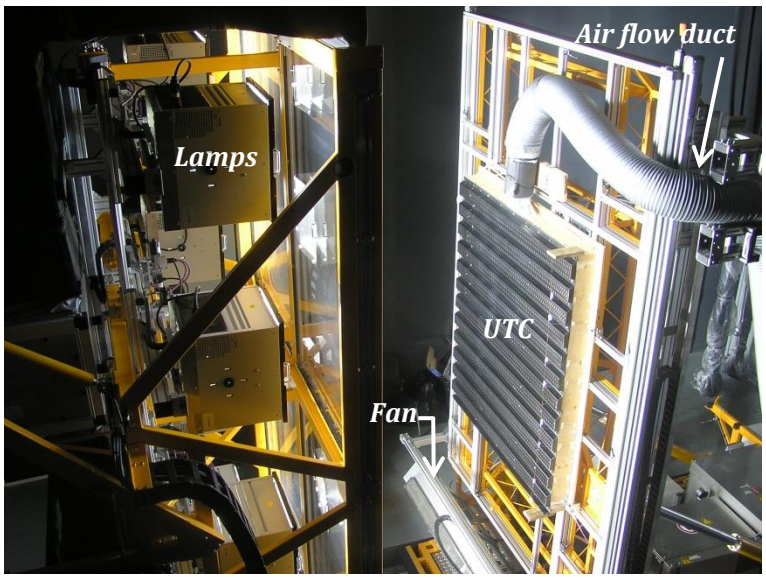

(b)

Figure 4.12: (a) Solar simulator in horozontal position

(b) UTC test panel mounted on the solar simulator frame in vertical position

CHAPTER 5

RESULTS AND DISCUSSION

The aim of this study was to examine the effect of wind direction on UTC performance, to assess the error in assuming uniform wind velocity distribution instead of the more realistic non-uniform distribution for analysis. For each proximity model case, four velocity distributions were studied – the assumed uniform distribution, where reference velocity V_{ref} is simply assumed to act normal to the surface and equally at all points with no regards to the wind direction, and the actual non-uniform distributions for the three wind directions For simplicity, it has been assumed that the UTC is flat not covered by PV panels unlike the actual JMSB solar-wall which is façade integrated PV/thermal wall.

5.1 *FULL-SCALE WIND VELOCITY DATA*

Full-scale wind data for a period of one year was obtained from the weather station located on the JMSB rooftop as well as the nearest airport weather station – Montreal Pierre Eliot Trudeau International Airport. The two data sets have been compared by means of wind-rose diagrams showing the distribution of wind speed and direction at the two stations (Figure 5.1).

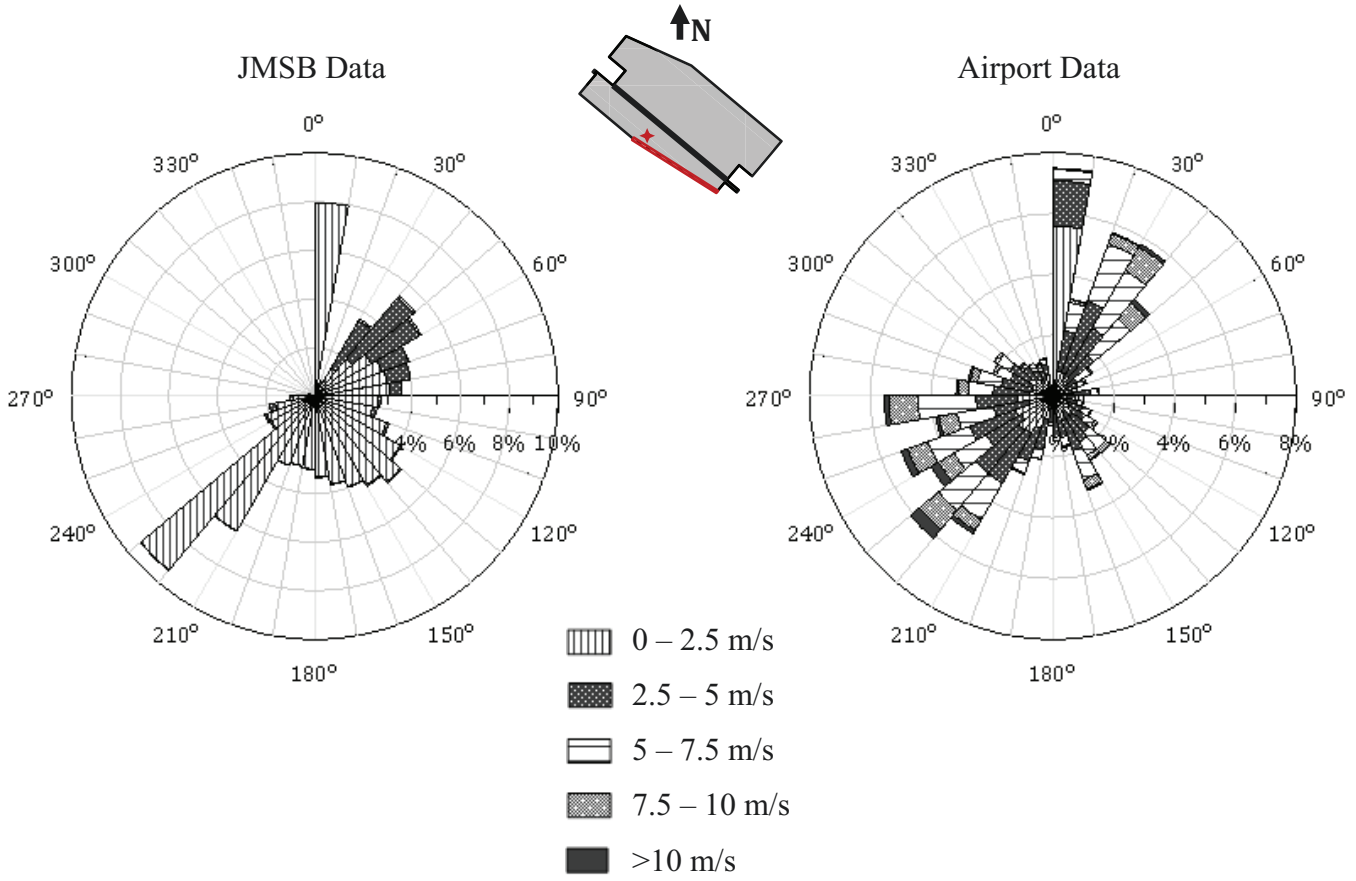

Figure 5.1: Wind-rose diagrams of full-scale wind data at JMSB and Montreal P.E.T International Airport

The data is divided into 10° sectors of the cardinal direction on the circumferential axis. The length of each sector, on the radial axis, represents the percentage of occurrences of wind from the particular direction. Each sector is further separated into wind speed ranges represented by the patterns shown in the legend.

It can be seen that the two data sets are in good agreement concerning wind directionality. As expected for an urban terrain (refer to Table 2.1) wind speeds at JMSB are, in general, lower than those recorded at the airport. Ideally, an anemometer would have to be set up where there is no obstruction to the oncoming wind. However, the JMSB anemometer is shielded in the cardinal directions from about 320° going clockwise to 120° by a large wall that is about 1 m taller than the anemometer (Figure 5.2).

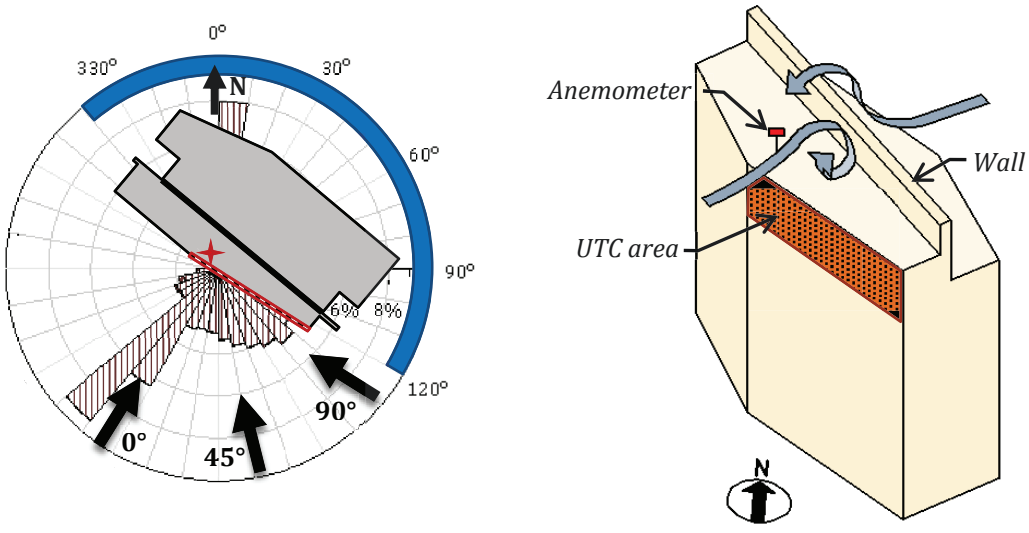

Figure 5.2: Sheltered wind directions and resulting flow pattern at the JMSB roof

This has two effects on the flow reaching the anemometer – wind approaching the building from this range of directions is obstructed by the wall and wind approaching from the front is intercepted by the wall and deflected back to the anemometer, most likely, at a higher speed than its approach. These phenomena result in erroneous readings and could be the reasons for high wind speeds in the cardinal sectors between 30° and 90° in the JMSB wind rose (see Figure 5.1). Therefore, although data from the two stations agree in their directionality, data recorded by the JMSB anemometer for the sheltered directions may not be entirely representative of the actual flow conditions. Since there is no way of judging which of the measurements were results of deflected flows, all measurements that corresponded to incidence angles greater than 90° were classified as leeward. Of the windward directions, predominant wind records were in the sector between Southeast and Southwest in light of which the three test directions were chosen as marked in Figure 5.2.

A scatter plot of the JMSB wind velocity data (Figure 5.3) shows that wind speeds at the JMSB roof for the windward directions are generally between 0.5 and 3 m/s with a major portion being of the order of 1 m/s and is representative of low wind conditions in the area. The highest wind speeds are of the order of 3 m/s.

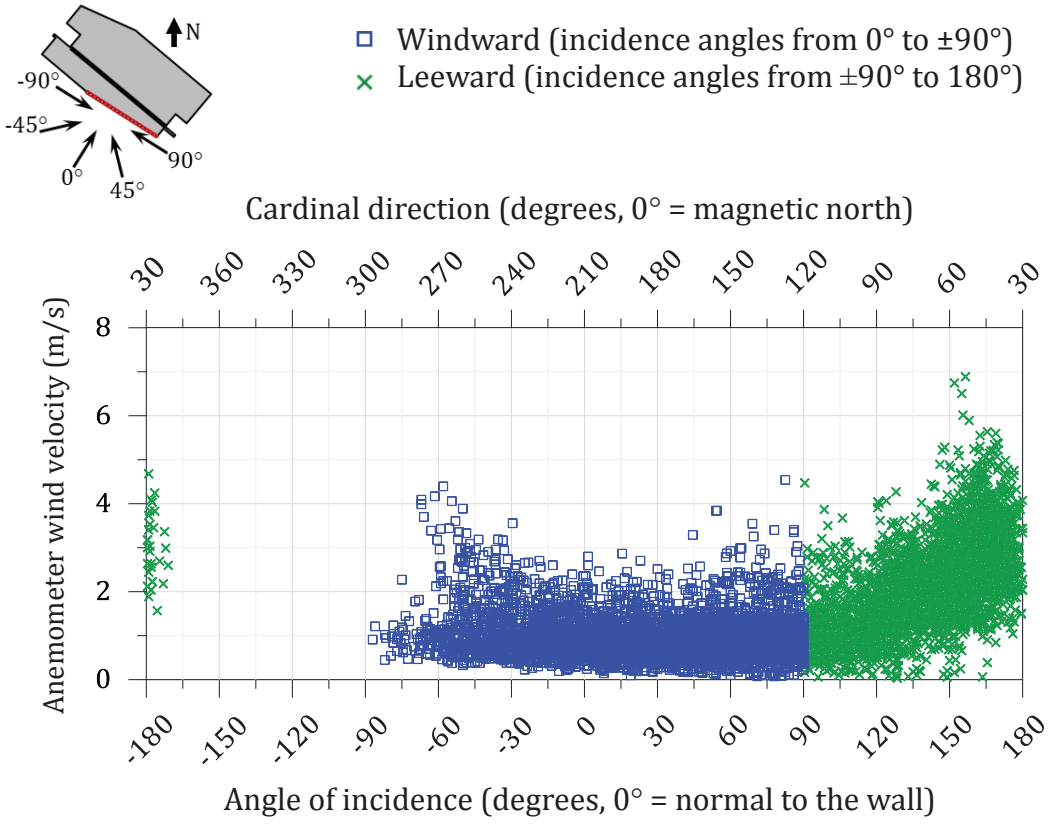

Figure 5.3: Hourly average wind velocity and direction on the JMSB roof for a period of one year [April 1, 2011 to March 31, 2012]

5.2 *WIND TUNNEL DATA*

5.2.1 *Local Velocity Distribution near the UTC Surface*

Wind tunnel experiments provided measurements of local velocity at 5 mm from the test area and 6.25 mm above the model roof. Since wind tunnel tests are done on scaled models of the subject, the best way to express these parameters is in the form of dimensionless figures. Therefore, the measurements are expressed as local velocity coefficients, defined as the ratio of the local wind velocity V_{loc} to the reference wind velocity V_{ref}. Figure 5.4 shows the contour plots of local velocity coefficients for the different cases and directions tested.

In general, mean speed reaching a target building would be lower in a developed area than what would be expected in an open area without as much blockage. However, the presence of other buildings at close proximity could result in higher local velocities due to complex wind-building interactions that have been discussed in Chapter 2. This is clearly reflected in the local velocity distributions for the two cases – higher values for Case 1 with the exception of 90° winds. The lower values for 90° in Case 1 are due to the fact that there are no tall structures in the Northwest that would influence the flow patterns as in the other directions. It can also be noted that the highest local velocities were for 45° winds; the high values persist over the entire test area and are not confined to the edges as in the case of normal winds. The results indicate local velocities near the edges of the test area that are up to 50% higher than the rooftop reference speed due to flow acceleration.

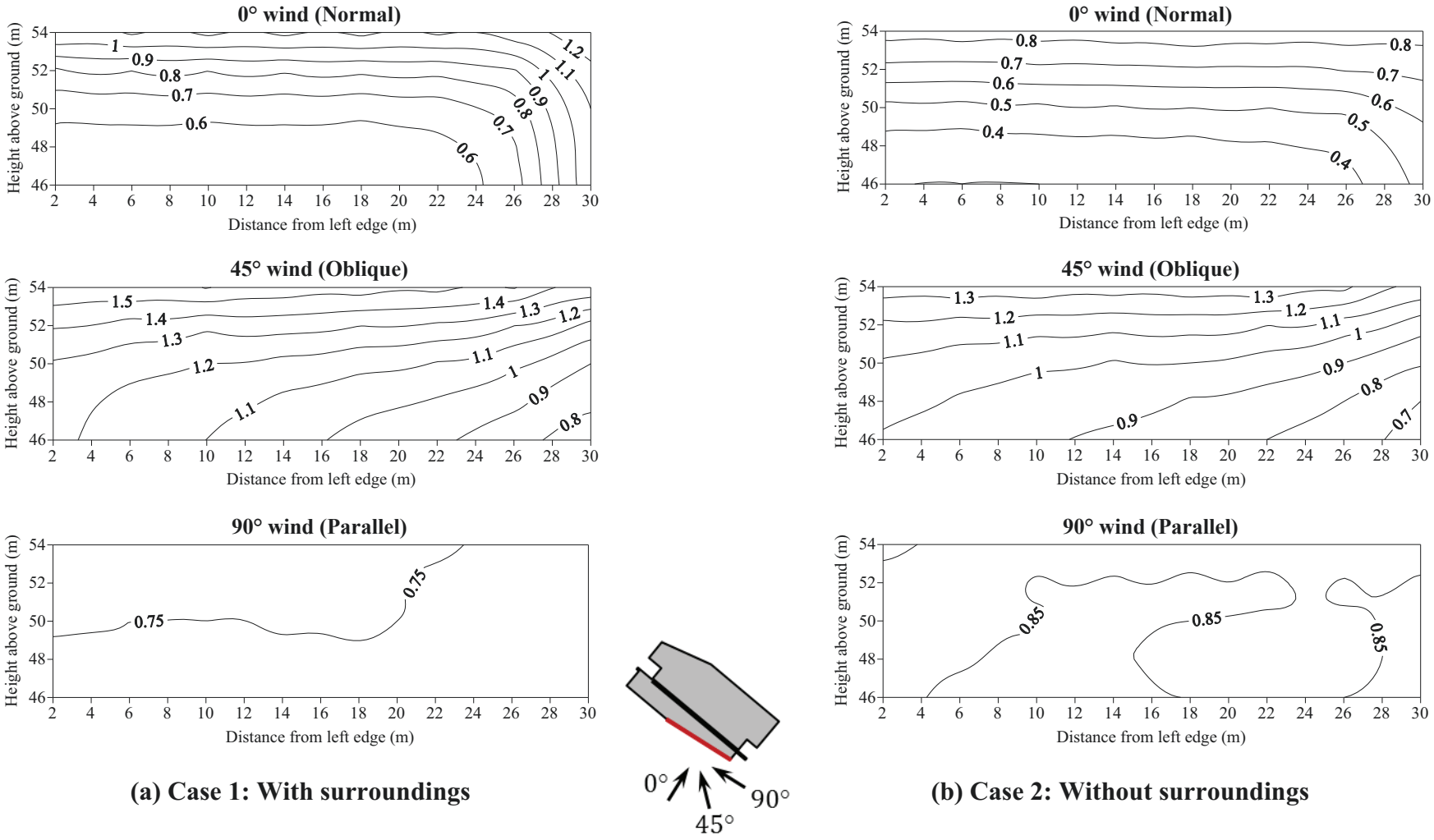

(a) Case 1: With surroundings

(b) Case 2: Without surroundings

Figure 5.4: Distribution of local velocity coefficients [V_{loc}/V_{ref}] over the test area

There is a general trend of the velocity coefficients in Case 2 being, on average, about 20% to 30% lower than in Case 1. This quantifies the impact of surrounding structures on the wind flow near the JMSB building.

For analysis using full-scale velocities, the local velocity V_{loc} for any point on the solar-wall area may easily be obtained by multiplying the corresponding velocity coefficient by the reference velocity. Typical wind speeds experienced by the JMSB building, from directions relevant to the UTC system, were found to be of the order of 1 m/s as recorded by the roof-mounted anemometer. Results in the following sections have been classified as pertaining to reference wind speeds of 1 m/s (low wind condition) and 3 m/s (high wind condition). These two values were chosen so as to be able to compare the results of this study with previous studies that were related to the JMSB solar-wall.

5.2.2 *Convective Heat Transfer Coefficient*

Since this study did not involve thermal measurements, CHTC h_c for the UTC was estimated by applying the experimental results of V_{loc}, described in the previous section, into analytical models relating CHTC to V_{loc}. In order to get the best approximation of CHTC, it is necessary to adopt models that were developed for experimental parameters similar to those used in the present study, the most important ones being wind velocity profile and direction. The CHTC-V_{loc} relations presented by Liu & Harris (2009) were the most detailed and specific to different

wind directions which made it more accurate than a generalized equation for a broad range of wind directions. The relations were developed from full-scale experiments on a single-storied building in open terrain. The test building in that study was oriented to face the predominant winds in the location; JMSB building also faces the predominant winds in Montreal (see Figure 4.9). The range of wind speeds experienced at the test area by that building (Liu & Harris, 2007) is similar to that at the top of the JMSB building which is located in an urban terrain. Such similarities made it reasonable to adopt the relations developed by Liu & Harris (2007) for the present analysis despite the two buildings being located in different exposure categories. The following relations (previously presented in section 3.3.1) were adopted in this study for the three wind directions tested:

$$h_c = 5.90V_{loc} + 3.95 \qquad 0° \tag{3-22}$$

$$h_c = 6.42V_{loc} + 3.17 \qquad 45° \tag{3-23}$$

$$h_c = 7.42V_{loc} + 2.98 \qquad 90° \tag{3-24}$$

For 45° and 90° directions, Liu & Harris (2009) have provided two expressions, one each for data measured for clockwise and counter-clockwise angles. This is due to the variation in the quantity of wind data obtained from different directions; ideally for a symmetrical structure, like the one Liu & Harris (2009) experimented on, the pattern of wind effects are symmetrical as well.

Therefore, expressions that were developed from a larger data set were chosen for the present study (see section 3.3.1).

CHTC was calculated at all measurement points by using the respective value of V_{loc} in equations (3-22) to (3-24) for the different wind directions and surrounding configurations. As for the uniform distribution case, since the assumption is that reference velocity acts uniformly over the entire UTC area, V_{loc} in the above equations was replaced by V_{ref}. The variation of surface-averaged CHTC with wind speed is shown in Figure 5.5. CHTC distribution on the UTC area would closely resemble the V_{loc} distribution owing to the linear relationship; the highest CHTC values corresponded to the highest wind velocities, i.e. for 45° winds. The error in surface-averaged CHTC as a result of using the assumed uniform velocity distribution in place of actual distributions for the three wind directions, presented in Table 5.1, were calculated as:

$$\%Error = \frac{Value\ for\ assumed\ distribution - Value\ for\ actual\ distribution}{Value\ for\ actual\ distribution} \times 100 \quad (5\text{-}1)$$

Positive values indicate an overestimation because of the assumption; larger the error, lower the CHTC for the actual distribution. Being representative of heat loss, it would be beneficial to have low CHTC for better UTC performance. Therefore, high negative values (high CHTC for actual distributions) may indicate the need for caution.

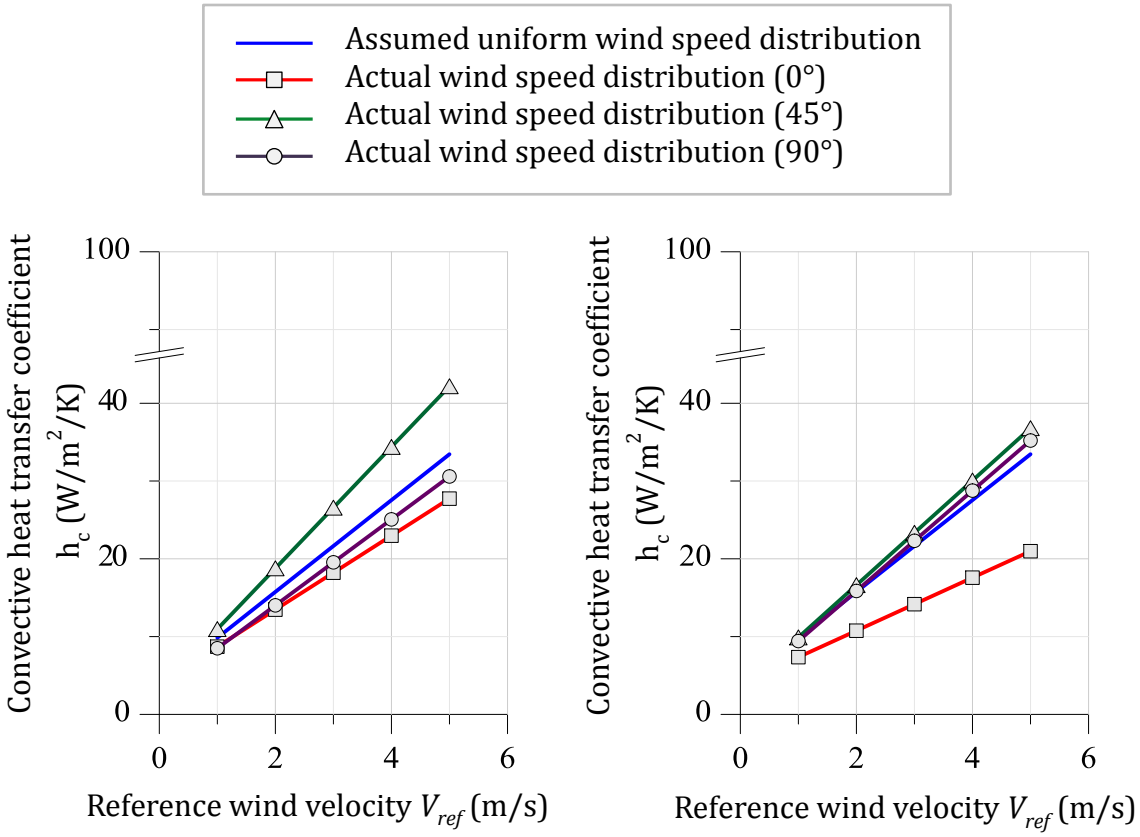

Figure 5.5: Comparison of convective heat transfer coefficients for different reference wind speeds and directions

Table 5.1: Error in surface-averaged CHTC due to uniform wind speed distribution assumption as compared to the results for actual directional distributions

Descriptor	Case 1: With surroundings		Case 2: Without surroundings	
	1 m/s	3 m/s	1 m/s	3 m/s
0° wind	13%	19%	34%	53%
45° wind	-10%	-19%	0%	-7%
90° wind	16%	11%	4%	-3%

Assuming that the reference speed acts normal to the surface at all points on the vertical facade, led to an overestimation of the surface-averaged CHTC by up to 16% for low wind speeds at 90° in Case 1. For the 45° direction however, results from the actual distribution are higher than the assumed case by 10% for low wind speeds and the error is almost double for high wind speed (19%); this warrants more attention. This is a direct result of the high local wind speeds corresponding to this angle of approach.

On comparing the results for Case 1 and Case 2, it can be inferred that the presence of surroundings seem to effect higher convection heat transfers due to the accelerated flows discussed in the previous section.

5.2.3 *UTC Plate Heat Exchange Effectiveness*

Heat exchange effectiveness ϵ is a parameter that represents the air heating ability of the absorber plate. It relates the outlet air temperature T_{back}, plate surface temperature T_{coll} and ambient air temperature T_{amb} as follows (recalled from section 3.2):

$$\epsilon = \frac{T_{back} - T_{amb}}{T_{coll} - T_{amb}} \tag{3-3}$$

Existing models for ϵ, developed as a function of wind velocity, assume that the wind acts normal to the UTC plate and the pores. For this reason V_{normal}, the normal component of V_{loc}, were used in the calculations of heat exchange

effectiveness ϵ. V_{normal} at each measurement point is the vector resolute of V_{loc} at that point to the building normal. The distributions of normal velocity coefficients – defined as the ratio of V_{normal} to the reference velocity V_{ref} – on the UTC area for the three wind directions are shown in Figure 5.6. Understandably, for every point, normal velocity coefficients are smaller than local velocity coefficients presented in Figure 5.4.

The following is the heat exchange effectiveness model, developed by Van Decker et al. (2001) and recalled from section 3.2, which was used in this study:

$$\epsilon = \left[1 - \left(1 + Re_s \, max\left[1.733 Re_w^{-\frac{1}{2}}, 0.02136\right]\right)^{-1}\right] \times \left[1 - \left(1 + 0.2273 Re_b^{\frac{1}{2}}\right)^{-1}\right] \times \exp\left(-0.01895 \frac{P}{D} - \frac{20.62}{Re_h} \frac{\mathrm{t}}{\mathrm{D}}\right) \quad (3\text{-}8)$$

where, Re is the Reynolds number, D and P are diameter and pitch of the UTC perforations and t is the plate thickness. In order to apply the velocity distributions to the heat exchange effectiveness model, the UTC wall was assumed to be composed of 40 individual collectors, each subjected to a different local wind velocity, represented by one measurement point and its tributary area – refer to Figure 4.10. The net effect of all 40 collectors working together in parallel was considered for overall plate heat exchange effectiveness ϵ.

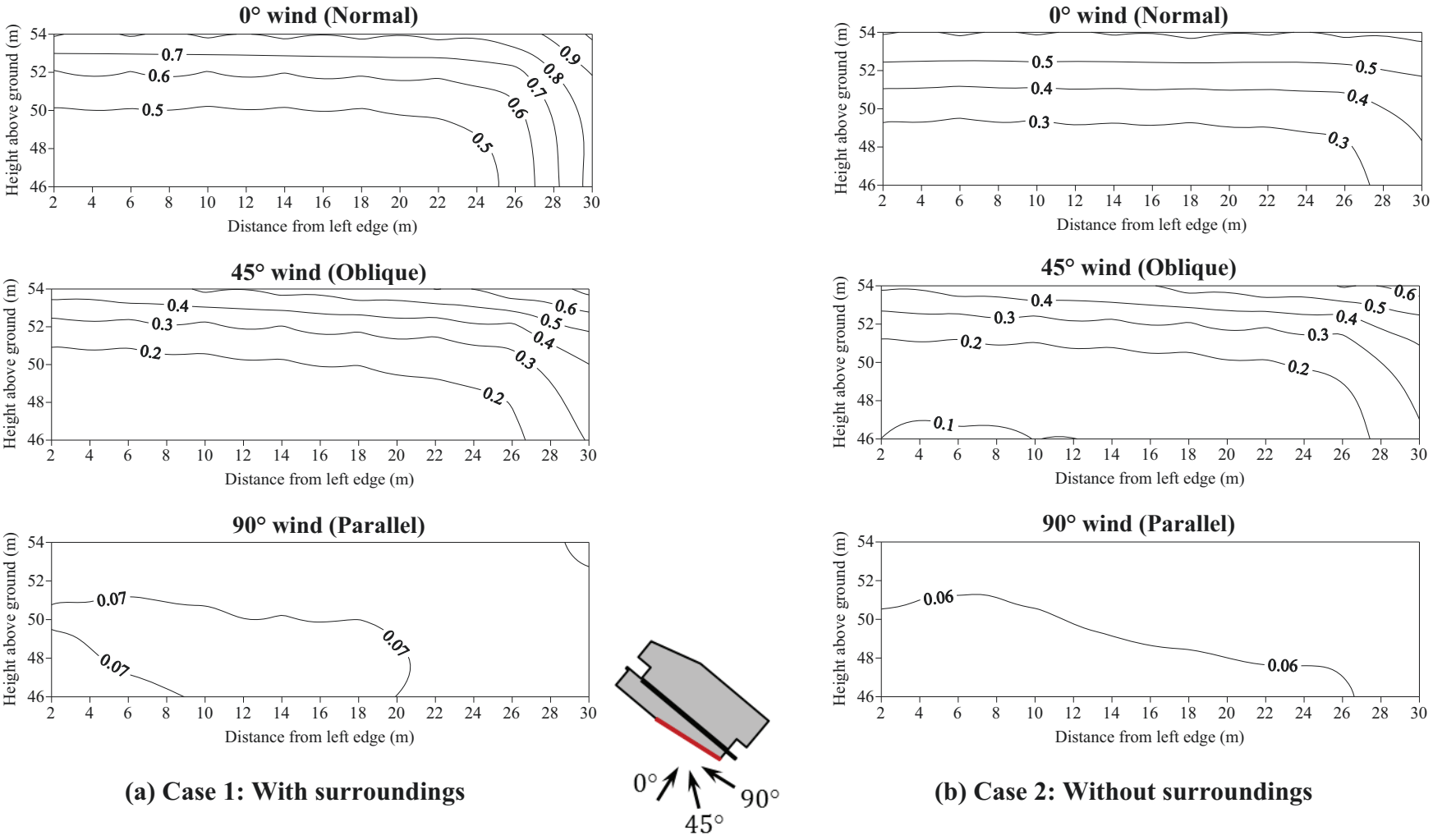

(a) Case 1: With surroundings

(b) Case 2: Without surroundings

Figure 5.6: Distribution of normal velocity coefficients [V_{normal}/V_{ref}] over the test area

Figure 5.7 shows the variation of ϵ for the different wind directions and the two proximity model cases tested. The effect of the normal velocity component of wind is to carry out the heat exchange more effectively. Therefore as expected, of the three wind directions, 0° wind is seen to effect maximum heat exchange as this orientation produces the largest normal velocity component. Farther the deviation of wind angle from the solar-wall normal, lower the resulting ϵ. The error in over-all heat exchange effectiveness as a result of the assumed uniform velocity distribution were calculated using equation (5-1) and are presented in Table 5.2. Larger the error, lower is the ϵ for actual distributions.

The interpretation of the errors for ϵ is different from that for CHTC in the previous section; while CHTCs are required to be low, high ϵ results in better UTC performance. Based on the results, the assumed distribution overestimates the effectiveness values in Case 1 for both low and high winds; the most significant differences are seen for parallel winds – 50% for low winds that are most prevalent in the JMSB area. On comparing the two cases it can be inferred that the presence of surroundings has very little effect – this is specific to the JMSB building, effects can vary for different buildings and surroundings. It can also be seen that with increase in free stream velocity, hence increase in normal velocity component, the effectiveness increases until it reaches a maximum beyond which the curve is asymptotical. This behavior is typical of perforated plates subjected to wind (Kutscher, 1994). Plate heat transfer effectiveness is a key factor in the prediction of UTC thermal efficiency; results pertaining to thermal efficiency are discussed in the following section.

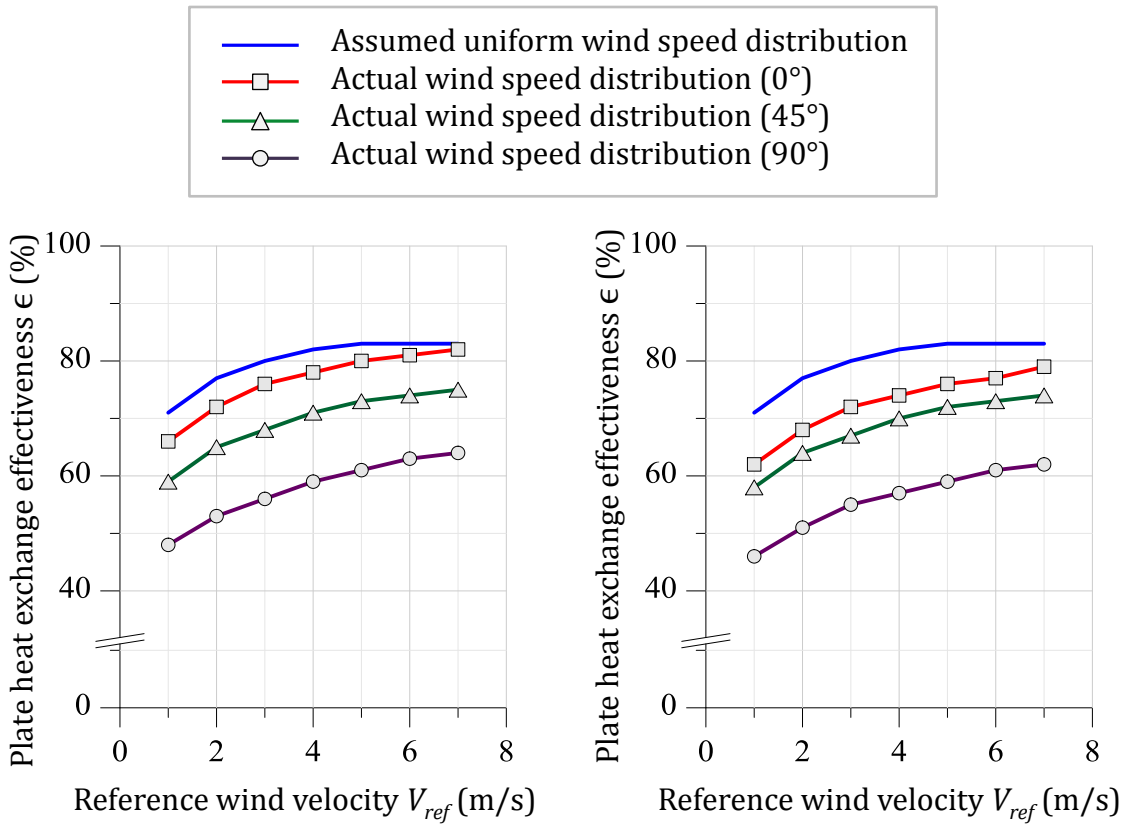

(a) With surroundings **(b) Without surroundings**

Figure 5.7: Comparison of heat exchange effectiveness for different reference wind speeds and directions

Table 5.2: Error in overall heat exchange effectiveness due to uniform wind speed distribution assumption as compared to the results for actual directional distributions

Descriptor	Case 1: With surroundings		Case 2: Without surroundings	
	1 m/s	3 m/s	1 m/s	3 m/s
0° wind	7%	6%	15%	12%
45° wind	21%	17%	24%	19%
90° wind	50%	43%	54%	48%

5.2.4 *UTC Thermal Efficiency*

Thermal efficiency η of a UTC defines how much of the available solar thermal energy it converts into useful form by heating air. Thermal efficiency model for UTC, developed by Kutscher et al. (1993), is recalled here from section 3.2:

$$\eta = \alpha_s \left[1 + \left(\frac{h_r}{\epsilon} + h_c\right)\left(\rho c_p V_s\right)^{-1}\right]^{-1} \tag{3-2}$$

Although the model has limitations due to the assumptions made in the study whereby it was developed (Kutscher, 1992; Kutscher et al., 1993), it is the most accurate model for UTC thermal efficiency available in literature.

Surface-averaged CHTC h_c (refer section 5.2.2) and over-all heat exchange effectiveness ϵ for the UTC (see section 5.2.3) calculated for different reference velocities and directional distributions for the two proximity model cases were applied to this equation; the results are presented in Figure 5.8. Highest values of η are seen for 0° winds which is the predominant wind direction for the JMSB location. "*Generally, and under typical operating conditions, a 10% (20%) error in predicting ϵ will produce a 5% (10%) error in predicting the efficiency…*" (Van Decker, et al., 2001). However, it can be seen from Figures 5.5, 5.7 and 5.8 that the variation of η with wind direction is more comparable to the trend followed by h_c than ϵ. For example, although 45° winds do not generate the lowest ϵ, this orientation provokes the highest h_c and the lowest η. Uniform velocity distribution assumption underestimates η for 0° and 90° corresponding to the overestimation of h_c for these

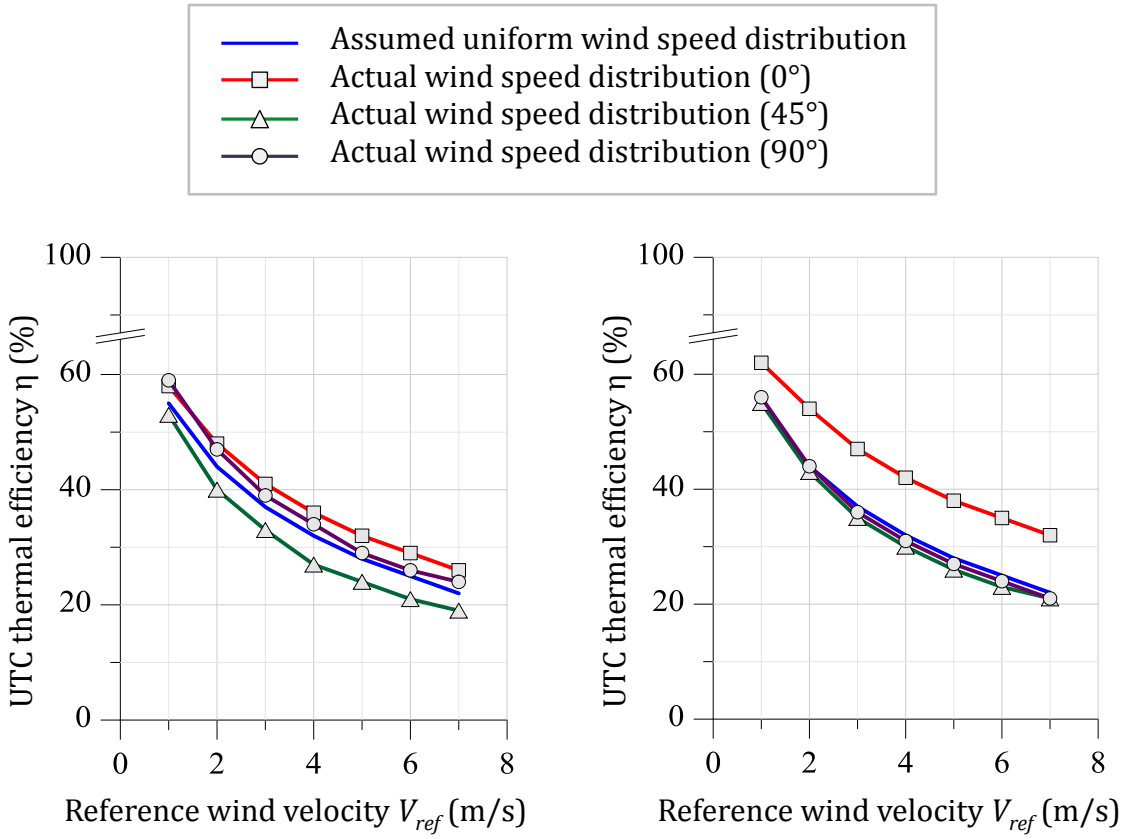

Figure 5.8: Comparison of thermal efficiency for different reference wind speeds and directions

Table 5.3: Error in thermal efficiency due to uniform wind speed distribution assumption as compared to the results for actual directional distributions

Descriptor	Case 1: With surroundings		Case 2: Without surroundings	
	1 m/s	3 m/s	1 m/s	3 m/s
0° wind	-5%	-11%	-11%	-22%
45° wind	4%	13%	0%	4%
90° wind	-6%	-6%	-2%	2%

directions. The inference is that UTC thermal efficiency is largely dependent on the convective heat loss term.

The errors in using the assumed distribution as opposed to actual directional distributions are shown in Table 5.3. The variability in directional wind speed distributions and the corresponding effects on h_c and ϵ seem to balance out in the prediction of thermal efficiency on which the wind direction seems to have very little effect. However, a notable feature, depicted by the graphs, is that thermal efficiency decreases with increasing wind speed – a reduction by 20 percentage points is seen for the range of wind speeds measured at JMSB (Between 1 and 3 m/s). For a UTC working under typical conditions at say, 50% efficiency in a geographic region receiving an average 800 W/m^2 of solar irradiance at peak hours, reduction of thermal efficiency to 30% would translate to about 160 W.hr/m^2 of heat loss through convection over an hour; calculated as follows:

$Thermal\ energy\ collected\ at\ 50\%\ efficiency\ Q_{50}$

$$= \frac{50}{100} \times 800 \frac{W}{m^2} \times 1hr = 400 \frac{W.hr}{m^2}$$

$Thermal\ energy\ collected\ at\ 30\%\ efficiency\ Q_{30}$

$$= \frac{30}{100} \times 800 \frac{W}{m^2} \times 1hr = 240 \frac{W.hr}{m^2}$$

Energy lost though convection is the difference between Q_{50} and Q_{30}

The 20 percentage point reduction is a direct difference between the η values corresponding to 1 and 3 m/s; it should not be confused with the percentage errors presented in Table 5.3 which were calculated using equation (5-1) to show the effect of wind direction.

5.3 *COMPARISON OF WIND TUNNEL AND SOLAR SIMULATOR RESULTS*

Bambara (2012) investigated the effect of wind on UTC in the solar simulator laboratory at Concordia University; experimental setup and procedure have been described in section 4.5. Flow parallel to the UTC was emulated by means of a fan. Results were presented for free stream wind speeds (V_∞) of 1 and 3 m/s, representing low and high wind conditions respectively.

Comparison between the results of the present study, corresponding to parallel wind distribution and assumed uniform normal distribution for reference wind speeds of 1 and 3 m/s, and the results of the solar-simulator study have been presented in Figure 5.9, which shows the variation of thermal efficiency as a function of air collection rate of the UTC. Air collection rate relates to the suction velocity V_s through the UTC pores as:

$$V_s = \frac{Air\ suction\ rate\ \left(\frac{kg}{hr.m^2}\right)}{\rho\left(\frac{kg}{m^3}\right) \times 3600(s)} \tag{5-2}$$

In addition to the observation that thermal efficiency of a UTC increases with increase in air collection rate (Bambara, 2012), it can also be seen from the two sets of graphs for the two reference wind speeds, that a wind speed increase from 1 to 3 m/s has the potential of decreasing the thermal efficiency by about 20 percentage points – this has been confirmed in the present study. Based on the comparison, the results of the present study are in close agreement with Bambara's results, which however are closer to the assumed uniform distribution case in the present study.

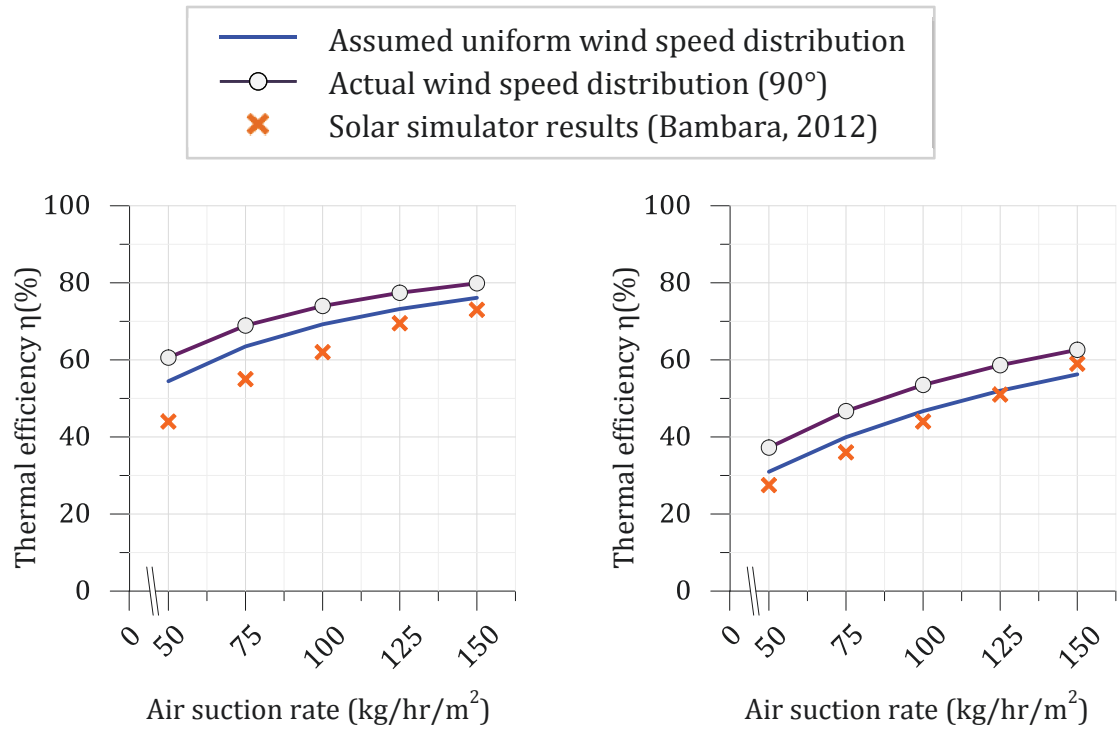

(a) Low wind speed V_∞=1 m/s **(b) High wind speed V_∞=3 m/s**

Figure 5.9: Comparison of thermal efficiency with solar simulator results for parallel wind

This was expected and in conformation with the assumption of uniform distribution in that study. Bambara assumed a parallel flow over the UTC based on the principle of bluff body aerodynamics and the presence of a stagnation point. However, this is true only for unobstructed approach wind on windward walls and most often not applicable for leeward walls. For buildings located in an urban setting, surrounded by other buildings of similar heights, this is seldom the case. The present study addresses this aspect with the inclusion of proximity models for more accurate flow simulation.

5.4 *PRACTICAL IMPLICATIONS AND COMPUTER SIMULATION*

As discussed in the previous sections, the most critical effect wind can have on UTC is the removal of useful heat leading to reduced thermal efficiency. This study presents an estimated reduction of thermal efficiency by 20 percentage points due to both wind speed and direction.

Most research studies in the past dealing with wind distribution on vertical walls were limited to terrain conditions with little or no obstruction to the flow. This is seldom the case in reality; local wind velocities and velocity distribution patterns are effects of the upstream terrain conditions and immediate surroundings of the concerned surface. Therefore existing correlations for local wind velocities, although broadly accepted for application to conditions similar to those they were developed in, cannot be generalized. Due to the case-specific nature of these correlations, it is advisable to use a combination of appropriate roughness lengths and scaled models of the immediate surroundings when simulating flow around buildings. This will allow for local wind turbulence and flow around surrounding structures to be better simulated as compared to the use of roughness length alone to generate the velocity profile. This measure is simpler in flow simulation programs where proximity models can be simulated as separate entities. However, in thermal simulation tools like DOE, ESP-R etc. where the external environment is simulated based on representative numerical inputs, the task of using accurate wind distributions may be difficult at this point. External coupling of flow and thermal simulation programs by which both domains may be synchronized and coupled (Djunaedy, et al., 2004; Mirsadeghi, et al., 2008) could be a way to get around this limitation.

CHAPTER 6

CONCLUSIONS AND RECOMMENDATIONS FOR FURTHER WORK

This study is an attempt to demonstrate the significance of using actual velocity distributions on large areas, as opposed to a single velocity value measured at a reference location, for UTC analyses. Velocity distribution on the solar-wall façade of the JMSB building was measured experimentally in a wind tunnel and a sensitivity study was done by applying the velocity distributions to performance evaluation models of UTCs. Proximity models were included in the wind tunnel tests to assess the impact of other structures in the vicinity on the wind velocity distributions. The following are the main conclusions from the study:

1. Actual directional distributions of wind velocity showed that local velocities, especially those near building edges, could be up to 50% higher than those measured above the roof owing to flow acceleration at these areas.
2. Winds at an incidence angle of 45° to the UTC were shown to have the greatest effect on CHTC and heat exchange effectiveness; CHTC values calculated were up to 19% higher than those for an assumed wind speed distribution and heat exchange effectiveness values were up to 50% lower for this orientation.
3. CHTC was found to have dominance over heat exchange effectiveness in the prediction of thermal efficiency.

4. Typical wind speeds measured at the JMSB rooftop were found to be between of the order of 1 m/s; high wind speeds were generally around 3 m/s. This range of wind speeds was found to reduce the UTC thermal efficiency by up to 20 percentage points.
5. Surrounding structures are seen to have a notable influence on the flow around the JMSB building; had there been no surrounding structures, the local wind velocities would have been about 20% - 30% lower than the prevalent conditions. The most significant effects were for 0° winds, which is the predominant direction in the JMSB area. Local flow patterns are highly dependent on the immediate surroundings and are very difficult to generalize. This emphasizes the importance of including proximity models in the wind related studies for more accurate simulation of the wind flow around the test building in both experimental and computational studies.

Although this study refers to a particular building – the JMSB – the qualitative results are expected to be applicable to other buildings in similar circumstances.

There have been very few studies in the past that aimed to develop direction specific correlations between UTC performance parameters and local wind speeds; existing correlations show little agreement with each other as they were developed for different experimental conditions. It would be interesting to see the development of more standardized correlations that would allow easier prediction and application of wind velocity distribution on building surfaces. A method to

incorporate terrain condition factors into these correlations is desirable for greater accuracy in estimation of local winds. Further investigation through full-scale studies and CFD modeling could provide detailed insights into the wind effects on UTC performance. An ideal study set-up would be one where the simulation functions of a wind tunnel and solar simulator could be combined to investigate the wind effects and corresponding thermal changes simultaneously.

The continual appraisal of technology and growing sophistication of control systems enables efficient management of energy flow in buildings. In order to maximize the functionality of such systems, there is constant need for greater accuracy in simulating real-world conditions.

REFERENCES

Athienitis, A. K., Bambara, J., O'Neill, B. & Faille, J., 2010. A prototype photovoltaic/thermal system integrated with transpired collector. *Solar Energy,* 85(1), pp. 139-153.

Augustus Leon, M. & Kumar, S., 2007. Mathematical modeling and thermal performance analysis of unglazed transpired solar collectors. *Solar Energy,* 81(1), pp. 62-75.

Bambara, J., 2012. *Experimental Study of a Façade-integrated Photovoltaic/thermal System,* M.A.Sc thesis: Concordia University, Montreal, Canada.

Blocken, B., Defraeye, T., Derome, D. & Carmeliet, J., 2009. High-resolution CFD simulations for forced convection heat transfer coefficients at the facade of a low-rise building. *Building and Environment,* 44(12), pp. 2396-2412.

CIBS, 1979. *Chartered Institute of Building Services Guide Book A, Section A3.* London: Cited in : Sharples, S., 1984. Full-scale measurements of convective energy losses from exterior building surfaces. *Building and Environment,* 19(1), pp. 31-39.

CIBSE, 2006. *Chartered Institute of Building Services Engineers Guide Book A, Section A3.* 7 ed. London: CIBSE.

Conserval Engineering Inc., n.d. *Company Info.* [Online]
Available at: http://solarwall.com
[Accessed 8 May 2012].

Cordeau, S. & Barrington, S., 2011. Performance of unglazed solar ventilation air pre-heaters for broiler barns. *Solar Energy,* 85(7), pp. 1418-1429.

Davenport, A. G., 1967. *The dependence of wind loads on meteorological parameters.* Ottawa, Proceedings of the International Conference on Wind Effects on Buildings and Structures: University of Toronto Press, pp. 19-82.

Defraeye, T., Blocken, B. & Carmeliet, J., 2010. CFD analysis of convective heat transfer at the surfaces of a cube immersed in a turbulent boundary layer. *International Journal of Heat and Mass Transfer,* 53(1-3), pp. 297-308.

Defraeye, T., Blocken, B. & Carmeliet, J., 2011. Convective heat transfer coefficients for exterior building surfaces: Existing correlations and CFD modelling. *Energy Conservation and Management,* 52(1), pp. 512-522.

Defraeye, T. & Carmeliet, J., 2010. A methodology to assess the influence of local wind conditions and building orientation on the convective heat transfer at building surfaces. *Environmental Modelling & Software,* 25(12), pp. 1813-1824.

Delisle, V., 2008. *Analytical and experimental study of a PV/thermal transpired solar collector,* PhD Thesis: University of Waterloo, Waterloo, Ontario.

Djunaedy, E., Hensen, J. L. M. & Loomans, M. G. L. C., 2004. *Comparing internal and external run-time coupling of CFD and building energy simulation software.* Coimbra, Portugal, Proceedings of the 9th ROOMVENT International Conference on Air Distribution in Rooms, 5-8 September 2004, University of Coimbra, pp. 393-396.

Dymond, C. & Kutscher, C., 1997. Development of a flow distribution and design model for transpired solar collectors. *Solar Energy,* 60(5), pp. 291-300.

Environment Canada, 2012. *National Climate Data and Information Archive.* [Online] Available at: http://climate.weatheroffice.gc.ca/climateData/canada_e.html [Accessed October 2012].

Fleck, B. A., Meier, R. M. & Matovic, M. D., 2002. A field study of the wind effects on the performance of an unglazed transpired solar collector. *Solar Energy,* 73(3), pp. 209-216.

Gawlik, K. M. & Kutscher, C. F., 2002. Wind heat loss from corrugated, transpired solar collectors. *Journal of Solar Energy Engineering,* 124(3), pp. 256-261.

Gunnewiek, L. H., Hollands, K. G. T. & Brundrett, E., 2002. Effect of wind on flow distribution in unglazed transpired-plate collectors. *Solar Energy,* 72(4), pp. 317-325.

Heinrich, M., 2007. *Transpired Solar Collectors - Results of a Field Trial,* Juddgeford, New Zealand: BRANZ Ltd.

Holmes, J. D., 2007. Wind loading of structures. In: New York, USA: Taylor & Francis, pp. 55-60.

Ito, N., Kimura, K. & Oka, J., 1972. A field experiment study on the convective heat transfer coefficient on exterior surface of a building. *ASHRAE Transactions,* 79(1), pp. 184-191.

Jürges , W., 1924. Der Wärmeübergang an einer ebenen Wand. *Beihefte zum Gesundheits-Ingenieur,* 1(19), pp. 1227-1249. Cited in : Sharples, S., 1984. Full-scale measurements of convective energy losses from exterior building surfaces. *Building and Environment,* 19(1), pp. 31-39.

Kutscher, C. F., 1992. *An investigation of heat transfer for air flow through low porosity perforated plates,* PhD Thesis: University of Colorado, Colorado, USA.

Kutscher, C. F., 1994. Heat exchange effectiveness and pressure drop for air flow through perforated plates with and without crosswind. *Journal of Heat Transfer,* 116(2), pp. 391-399.

Kutscher, C. F., Christensen, C. B. & Barker, G. M., 1993. Unglazed transpired solar collectors: heat loss theory. *Journal of Solar Energy Engineering,* 115(3), pp. 182-188.

Liu, Y. & Harris, D. J., 2007. Full-scale measurements of convective coefficient on external surface of a low-rise building in sheltered conditions. *Building and Environment,* 42(7), pp. 2718-2736.

Loveday, D. L. & Taki, A. H., 1996. Convective heat transfer coefficients at a plane surface on a full-scale building facade. *International Journal of Heat and Mass Transfer,* 39(8), pp. 1729-1742.

Mirsadeghi, M., Blocken, B. & Hensen, J. L. M., 2008. *Validation of external BES-CFD coupling by inter-model comparison.* Kyoto, Japan. In Murakami, S (Ed.), 29th AIVC Conference, 14-16 October 2008, pp. 193-198.

Moore, R., 2005. *Solar air heating and cooling,* Camberwell, Australia: ISS Institute Inc..

Morse, E. S., 1881. *Warming and ventilating apartments by the sun's rays.* Massachusetts, U.S.A, Patent No. 246626.

NRCan, 2010. *Solar Thermal.* [Online]
Available at: http://canmetenergy.nrcan.gc.ca
[Accessed 15 November 2012].

NREL, 1998. *Transpired Collectors (Solar Preheaters for Outdoor Ventilation Air),* Golden, Colorado: U.S. Department of Energy.

O'Neill, B., Chen, Y. & Koziol, A., 2011. *Description of the JMSB BIPV/T solar system, monitoring and database,* Solar Buildings Research Network: Concordia University, Montreal.

REN21, 2012. *Renewables 2012 Global Status Report,* Paris: REN21 Secretariate.

R. M. Young Company, n.d. *Wind Monitor.* [Online]
Available at: http://www.youngusa.com/products/7/8.html
[Accessed 20 December 2012].

Shao, J. et al., 2010. Field measurement of the convective heat transfer coefficient on vertical external building surface using naphthalene sublimation method. *Journal of Building Physics,* 33(4), pp. 307-326.

Sharples, S., 1984. Full-scale measurements of convective energy losses from exterior building surfaces. *Building and Environment,* 19(1), pp. 31-39.

Simiu, E., 1981. Modern developments in wind engineering : Part 1. *Engineering Structures,* 3(4), pp. 233-241.

Stathopoulos, T., 1984. Design and fabrication of a wind tunnel for building aerodynamics. *Journal of Wind Engineering and Industrial Aerodynamics,* 16(2-3), pp. 361-376.

Stathopoulos, T., 2007. In: T. Stathopoulos & C. C. Baniotopoulos, eds. *Wind effects on buildings and design of wind-sensitive structures.* International Center for Mechanical Sciences, Udine, Italy: Springer Wien New York, pp. 1-15.

Test, F. L., Lessmann, R. C. & Johary, A., 1981. Heat transfer during wind flow over rectangular bodies in the natural environment. *Journal of Heat Transfer,* 103(2), pp. 262-267.

Van Decker, G. W. E., Hollands, K. G. T. & Brunger, A. P., 2001. Heat-exchange relations for unglazed transpired solar collectors with circular holes on a square or triangular pitch. *Solar Energy,* 71(1), pp. 33-45.

Vasan, N. & Stathopoulos, T., 2012. *Wind Tunnel Assessment of the Wind Velocity Distribution on.* Halifax, Canada, Proceedings of eSim 2012: The Canadian Conference on Building Simulation, 1-4 May, pp. 61-74.